



HAL
open science

Biallelic NFATC1 mutations cause an inborn error of immunity with impaired CD8+ T-cell function and perturbed glycolysis

Sevgi Kostel Bal, Sarah Giuliani, Jana Block, Peter Repiscak, Christoph Hafemeister, Tala Shahin, Nurhan Kasap, Bernhard Ransmayr, Yirun Miao, Cheryl van de Wetering, et al.

► **To cite this version:**

Sevgi Kostel Bal, Sarah Giuliani, Jana Block, Peter Repiscak, Christoph Hafemeister, et al.. Biallelic NFATC1 mutations cause an inborn error of immunity with impaired CD8+ T-cell function and perturbed glycolysis. *Blood*, 2023, 142 (9), pp.827-845. 10.1182/blood.2022018303 . hal-04309057

HAL Id: hal-04309057

<https://amu.hal.science/hal-04309057v1>

Submitted on 27 Nov 2023

HAL is a multi-disciplinary open access archive for the deposit and dissemination of scientific research documents, whether they are published or not. The documents may come from teaching and research institutions in France or abroad, or from public or private research centers.

L'archive ouverte pluridisciplinaire **HAL**, est destinée au dépôt et à la diffusion de documents scientifiques de niveau recherche, publiés ou non, émanant des établissements d'enseignement et de recherche français ou étrangers, des laboratoires publics ou privés.

Biallelic *NFATC1* mutations cause an inborn error of immunity with impaired CD8⁺ T-cell function and perturbed glycolysis

Tracking no: BLD-2022-018303R2

Sevgi Kostel Bal (Ludwig Boltzmann Institute for Rare and Undiagnosed Diseases, Austria) Sarah Giuliani (St. Anna Children's Cancer Research Institute (CCRI), Austria) Jana Block (St Anna Children's Cancer Research Institute (CCRI), Austria) Peter Repiscak (St. Anna Children's Cancer Research Institute (CCRI), Austria) Christoph Hafemeister (St. Anna Children's Cancer Research Institute (CCRI), Austria) Tala Shahin (St. Anna Children's Cancer Research Institute (CCRI), Austria) Nurhan Kasap (Marmara University, Division of Allergy and Immunology, Turkey) Bernhard Ransmayr (St. Anna Children's Cancer Research Institute (CCRI), Austria) Yirun Miao (St. Anna Children's Cancer Research Institute (CCRI), Austria) Cheryl van de Wetering (St. Anna Children's Cancer Research Institute (CCRI), Austria) Raul Jimenez-Heredia (St. Anna Children's Cancer Research Institute (CCRI), Austria) Michael Schuster (CeMM Research Center for Molecular Medicine of the Austrian Academy of Sciences, Austria) Samaneh Zoghi (St. Anna Children's Cancer Research Institute (CCRI), Austria) Vanessa Hertlein (St. Anna Children's Cancer Research Institute (CCRI), Austria) Marini Thian (DSRE, Takeda Pharmaceuticals International Co., United States) Aleksandr Bykov (St. Anna Children's Cancer Research Institute (CCRI), Austria) Royala Babayeva (Division of Pediatric Allergy and Immunology, Turkey) Sevgi Bilgic Eltan (Marmara University, Division of Allergy and Immunology, Turkey) Elif Karakoc-Aydiner (Marmara University, Research and Training Hospital,) Lisa Shaw (Medical University Vienna, Austria) Iftekhar Chowdury (Institute of Biotechnology, Finland) Markku Varjosalo (Institute of Biotechnology, Finland) Rafael Argüello (Aix Marseille Univ, France) Matthias Farlik (CeMM Research Center for Molecular Medicine, Austria) Ahmet Ozen (Division of Pediatric Allergy and Immunology, Turkey) Edgar Serfling (Institute of Pathology, Germany) Loïc Dupré (Ludwig Boltzmann Institute for Rare and Undiagnosed Diseases, Austria) Christoph Bock (CeMM Research Center for Molecular Medicine of the Austrian Academy of Sciences, Austria) Florian Halbritter (St. Anna Children's Cancer Research Institute (CCRI), Austria) J. Thomas Hannich (Research Center for Molecular Medicine of the Austrian Academy of Sciences (CeMM), Vienna, Austria, Austria) Irinka Castanon (St. Anna Children's Cancer Research Institute (CCRI), Austria) Michael Kraakman (Ludwig Boltzmann Institute for Rare and Undiagnosed Diseases, Austria) Safa Baris (Marmara University, Faculty of Medicine, Turkey) Kaan Boztug (Ludwig Boltzmann Institute for Rare and Undiagnosed Diseases, Austria)

Abstract:

The NFAT family of transcription factors plays central roles in adaptive immunity in murine models, however, their contribution to human immune homeostasis remains poorly defined. In a multigenerational pedigree, we identified three patients carrying germline biallelic missense variants in *NFATC1*, presenting with recurrent infections, hypogammaglobulinemia and decreased antibody responses. The compound heterozygous *NFATC1* variants identified in the patients caused decreased stability and reduced binding of DNA and interacting proteins. We observed defects in early activation and proliferation of T and B cells from these patients, amenable to reconstitution upon genetic rescue. Following stimulation, T-cell activation and proliferation were impaired, reaching that of healthy controls with delay indicative of an adaptive capacity of the cells. Assessment of the metabolic capacity of patient T cells, revealed that NFATc1-dysfunction rendered T cells unable to engage in glycolysis following stimulation, although oxidative metabolic processes were intact. We hypothesized that NFATc1-mutant T cells could compensate for the energy deficit due to defective glycolysis by enhanced lipid metabolism as an adaptation, leading to a delayed, but not lost activation responses. Indeed, we observed increased ¹³C-labelled palmitate incorporation into citrate indicating higher fatty acid oxidation and we demonstrated that metformin and rosiglitazone improved patient T-cell effector functions. Collectively, enabled by our molecular dissection of *NFATC1* mutations and extending the role of NFATc1 in human immunity beyond receptor signaling, and reveal evidence of metabolic plasticity in the context of impaired glycolysis observed in patient T cells to remedy delayed effector responses.

Conflict of interest: No COI declared

COI notes:

Preprint server: No;

Author contributions and disclosures: S.K.B. performed most of the experiments on patient material, analyzed and interpreted the patient and experimental data. S.K.B., S.G, J.B. and T.S., performed the biochemical experiments, with help from VH. S.K.B. supervised S.G. M.K. and S.K.B. planned the metabolism experiments, performed and analyzed them together, with technical assistance of S.G. M.S. analyzed the RNA-seq data under supervision of C.B. P.R. analyzed the RNAseq and ATACseq data. CH analyzed the scRNA-seq data and rerun the pipeline for the ATACseq under the supervision of F.H. R.J.H. identified the variant, run the WES, ATACseq and RNA-seq prep; A.F. performed the segregation analysis and protein conservation analysis, and qPCR experiments. I.C. and M.V. gave intellectual input. J.B. assisted in imaging analysis and provided critical intellectual input. S.K.B. and B.R. prepared samples and interpreted the scRNA-seq results together. B.R. performed the B-cell activation, proliferation and class switch experiments. Y.M. assisted in tissue culture of T cells and performing imaging experiments. CvdW run WB for co-IP experiments, assisted in the data analysis of hexokinase assay, provided intellectual input and controlled manuscript. S.Z. assisted in tissue culture of B cells and transfection of EBV B-cells. M.T. assisted in the B cell class switch assays. A.B. reran the pipeline for RNAseq experiments and replotted the GSEA graphs. L.E.S. performed scRNA sequencing under the supervision of M.F. S.B. recruited the patients in Turkey supervised the patient follow-ups, N.K., R.B., S.B.E., E.K., A.O. followed the patients and assisted in the collection of medical data. R.A. provided the necessary material, protocol and consultancy for SCENITH experiments. L.D. provided protocols and consultancy for the T cell functional experiments (T-cell expansion, imaging and degranulation). T.H. ran the MS for metabolomics, lipidomics and fluxomics and made the initial data analysis. S.K.B., M.K., I.C.O. and K.B. wrote the manuscript with input from all co-authors. K.B. conceptualized and coordinated the study, provided laboratory resources, and took overall responsibility of the study.

Non-author contributions and disclosures: No;

Agreement to Share Publication-Related Data and Data Sharing Statement: Processed single-cell RNA-seq data are going to be openly available via Gene Expression Omnibus (GEO, accession number pending). Raw sequencing reads are going to be available under controlled access via the European Genome-Phenome Archive (EGA, accession number pending) to safeguard patient privacy. R code used for the analysis for single-cell RNA-seq data are going to be available via GitHub: <https://github.com/cancerbits/nfatc1>. Raw data from LC-MS will be available in Massive (identifier number pending)

Clinical trial registration information (if any):

Biallelic *NFATC1* mutations cause an inborn error of immunity with impaired CD8⁺ T- cell function and perturbed glycolysis

Sevgi Kostel Bal^{1,2}, Sarah Giuliani^{1,2}, Jana Block^{1,2,3}, Peter Repiscak¹, Christoph Hafemeister¹, Tala Shahin^{1,2,3}, Nurhan Kasap^{4,5}, Bernhard Ransmayr^{1,2,3}, Yirun Miao^{1,2,3}, Cheryl van de Wetering¹, Alexandra Frohne^{1,2}, Raul Jimenez Heredia^{1,2}, Michael Schuster³, Samaneh Zoghi^{1,2}, Vanessa Hertlein^{1,2,3}, Marini Thian^{1,2}, Aleksandr Bykov¹, Royala Babayeva^{4,5}, Sevgi Bilgic Eltan^{4,5}, Elif Karakoc Aydiner^{4,5}, Lisa E. Shaw⁶, Iftekhar Chowdhury⁷, Markku Varjosalo⁷, Rafael J. Argüello⁸, Matthias Farlik⁷, Ahmet Ozen^{4,5}, Edgar Serfling⁹, Loic Dupre^{2,7,10}, Christoph Bock^{2,3,11}, Florian Halbritter¹, J. Thomas Hannich³, Irinka Castanon^{1,2}, Michael J. Kraakman^{1,2}, Safa Baris^{4,5#}, Kaan Boztug^{1,2,3,12,13#}

SB and KB contributed equally.

¹ St. Anna Children's Cancer Research Institute (CCRI), Vienna, Austria

² Ludwig Boltzmann Institute for Rare and Undiagnosed Diseases, Vienna, Austria

³ CeMM Research Center for Molecular Medicine of the Austrian Academy of Sciences, Vienna, Austria

⁴ Division of Pediatric Allergy and Immunology, Marmara University, Istanbul, Turkey

⁵ The Isil Berat Barlan Center for Translational Medicine, Division of Pediatric Allergy and Immunology, Marmara University, Istanbul, Turkey

⁶ Department of Dermatology, Medical University of Vienna, Vienna, Austria

⁷ Institute of Biotechnology, University of Helsinki, Helsinki, Finland

⁸ Aix Marseille Univ, CNRS, INSERM, CIML, Centre d'Immunologie de Marseille- Luminy, Marseille, France

⁹ Department of Molecular Pathology, Institute of Pathology, and Comprehensive Cancer Center Mainfranken, University of Würzburg, Würzburg, Germany.

¹⁰ Toulouse Institute for Infectious and Inflammatory Diseases (INFINITY), INSERM, CNRS, Toulouse III Paul Sabatier University, Toulouse, France

¹¹ Medical University of Vienna, Institute of Artificial Intelligence, Center for Medical Data Science, Vienna, Austria

¹² St. Anna Children's Hospital, Vienna, Austria

¹³ Medical University of Vienna, Department of Pediatrics and Adolescent Medicine, Vienna, Austria

Corresponding author:

Kaan Boztug MD

St. Anna Children's Cancer Research Institute (CCRI)

Zimmermannplatz 10, A- 1090 Vienna, Austria

Phone: +43 1- 40470- 4080 Fax:

+43- 1- 40170- 7280

e- mail: kaan.boztug@ccri.at

Manuscript word counts: 4000

Abstract word count: 243

Figure count: 7

Reference count: 61

Key points

- Germline biallelic loss- of- function mutations in *NFATC1* underly a previously unknown inborn error of immunity.
- NFATc1 defects curtail the activation responses of CD8⁺ cytotoxic T cells due to impaired glycolysis.
- CD8⁺ T cells with NFATc1 dysfunction adapt to impaired glycolysis likely by fostering fatty acid utilization.

Abstract

The NFAT family of transcription factors plays central roles in adaptive immunity in murine models, however, their contribution to human immune homeostasis remains poorly defined. In a multigenerational pedigree, we identified three patients carrying germline biallelic missense variants in *NFATC1*, presenting with recurrent infections, hypogammaglobulinemia and decreased antibody responses. The compound heterozygous *NFATC1* variants identified in the patients caused decreased stability and reduced binding of DNA and interacting proteins. We observed defects in early activation and proliferation of T and B cells from these patients, amenable to reconstitution upon genetic rescue. Following stimulation, T- cell activation and proliferation were impaired, reaching that of healthy controls with delay indicative of an adaptive capacity of the cells. Assessment of the metabolic capacity of patient T cells, revealed that NFATc1- dysfunction rendered T cells unable to engage in glycolysis following stimulation, although oxidative metabolic processes were intact. We hypothesized that NFATc1- mutant T cells could compensate for the energy deficit due to defective glycolysis by enhanced lipid metabolism as an adaptation, leading to a delayed, but not lost activation responses. Indeed, we observed increased ¹³C- labelled palmitate incorporation into citrate indicating higher fatty acid oxidation and we demonstrated that metformin and rosiglitazone improved patient T- cell effector functions. Collectively, enabled by our molecular dissection of *NFATC1* mutations and extending the role of NFATc1 in human immunity beyond receptor signaling, and reveal evidence of metabolic plasticity in the context of impaired glycolysis observed in patient T cells to remedy delayed effector responses.

Keywords: NFATc1, CD8 T- cell metabolism, metabolic reprogramming, metabolic plasticity, inborn errors of immunity

Introduction

T cells can possess a diverse spectrum of functional states, governed primarily by cues in their environment. Hence, T cells constantly fine-tune their behavior through coordination between signal transduction pathways, gene expression and cellular metabolism. Studying how metabolic circuitries contribute to T-cell responses is fundamental to our understanding of the immune system and currently under intense scrutiny^{1,2}. However, most studies have been conducted within the field of chronic inflammation and tumor immunity and typically focus on components within metabolic pathways. Consequently, the contribution of transcriptional regulation to metabolic control within T cells, particularly in the context of human disease remains poorly understood.

The nuclear factor-of-activated T cells (NFAT) family of transcription factors (TF) regulates T-lymphocyte activation, survival, proliferation and differentiation, as well as the transcription of many growth factors, cytokines, and cell-to-cell interaction molecules that are essential for the morphogenesis, development, and function of numerous cell types and organ systems³⁻⁵. The NFAT family comprises five members of which NFATc1, NFATc2, and NFATc3 are strongly expressed in lymphocytes⁵. In T- and B-cells, stimulation of the antigen receptor (TCR and BCR, respectively) triggers signaling cascades resulting in Ca^{2+} -release from the endoplasmic reticulum (ER) to the cytosol. Decreased Ca^{2+} in the ER lumen is sensed by stromal interaction molecules (STIM) that activate pore-forming ORAI proteins at the plasma membrane and induce store-operated Ca^{2+} entry (SOCE)⁵⁻⁷. Increased cytoplasmic Ca^{2+} leads to the activation of calcineurin, which subsequently dephosphorylates NFATc⁵. Upon dephosphorylation, cytoplasmic NFATc translocates to the nucleus where it regulates gene transcription in cooperation with various other TFs such as AP-1, a heterodimer consisting of Jun and Fos members⁵⁻⁷.

Distinct roles of individual NFATc members have been shown in murine T lymphocytes, particularly during differentiation of Th17, T-follicular helper cells (Tfh) and regulatory T cells (Tregs)³. Perturbations in NFATc activity, via loss of binding to AP-1, are linked to CD8⁺ T-cell exhaustion upon prolonged stimulation in models of chronic infection and oncogenesis⁸.

Recently, NFATc1 has been discovered as a central regulator of T-cell metabolism. Under physiological conditions, activated CD8⁺ T cells shift their metabolism from

oxidative phosphorylation (OXPHOS) to glycolysis. Dysfunctions of SOCE/NFAT axis rendered mouse T cells fail to undergo the glycolytic switch necessary for metabolic expenses during activation

and clonal expansion^{9,10}. Here, we report two heterozygous loss- of- function (LOF) mutations in compound heterozygosity in *NFATC1* as the etiology of a previously unknown inborn error of immunity (IEI). We dissect the molecular function of NFATc1, as a TF and extend its role beyond receptor signaling. Specifically, we demonstrate that NFATc1 is required for intact glycolytic metabolism, revealing the fundamental but permissive nature of metabolic circuitries in governing T- cell responses in an IEI setting. In addition, we demonstrate that NFATc1- dysfunctional T cells **shift towards alternative metabolic resources such as** fatty acid (FA) utilization and showcase the exploitability of this phenomenon in patient cells with the use of metformin and rosiglitazone providing proof- of- concept for therapeutic modulation of immunometabolic states to improve effector functions in a genetically defined T- cell defect.

Material and methods

Study approval

Samples from the patients, family members and other healthy controls (HCs) were obtained following an informed written consent and approval from the ethics committee of Marmara University Faculty of Medicine as well as the Institutional Review Board of the Medical University of Vienna.

Whole exome sequencing (WES)

For WES, a TrueSeq Rapid Exome kit as well as the Illumina HiSeq3000 system and the cBot cluster generation instruments were used as previously described¹¹. A detailed list of genetic variants is shown in Supplementary Tables 2- 6.

Immunoblot experiments

Immunoblots were done according to established protocols as outlined¹¹.

Lymphocyte phenotyping and functions

Cryopreserved PBMCs were stained with fluorescent antibodies (Supplementary Table 1). PBMCs or sorted CD8⁺ T- cell subsets were isolated and cultured *in vitro* under various conditions¹¹ and proliferation, activation, cytokine expression, or apoptosis were determined. Data were acquired with an LSRFortessa™ (BD Biosciences) and analyzed using FlowJo™ v.10. The gating strategies and the panels are shown in Supplementary Figure 1 and Supplementary Table 1 respectively.

Treatment of T- lymphoblasts with metformin and rosiglitazone

Patient and HC T cells were expanded as described¹¹. Starting on day 5 after the initial stimulation, metformin (2mM; Sigma) or rosiglitazone (1 μM; Sigma) or carrier were added until day 10, when the experiments were performed.

Statistical analysis

For single comparisons of independent groups, Student's t test was performed. For multiple comparisons, a one or two- way analysis of variance (ANOVA) followed by corrections of multiple tests were applied. Analyses were performed using PRISM software (GraphPad Software Inc).

Results

Identification of human *NFATC1* mutations

Here we studied 3 patients (P1- P3) from a multigenerational consanguineous pedigree (Figure 1A), who suffered from early- onset sinopulmonary infections requiring multiple hospitalizations and eventually leading to bronchiectasis. In the extended family, we noted that several infants (from whom no genetic material was available for testing) succumbed to infectious complications (Supplementary information). P2 and P3 experienced recurrent viral (warts) and bacterial (folliculitis and abscesses) skin infections. Thoracolumbal scoliosis was documented in P1 and P2, which was corrected by surgery (Figure 1B). Laboratory results indicated hypogammaglobulinemia (more prominently in P1) and low antibody titers following pneumococcus vaccine were detected in P1. P3 had negative response to hepatitis B vaccine. (Supplementary Table 2). Immunophenotyping revealed lower CD4⁺/CD8⁺ T- cell ratio and lower recent thymic emigrants compared with the age- matched controls. Lymphocyte proliferation responses to PHA and CD3/CD28 stimulations were defective (Supplementary Table 2). At present, P1 and P2 receive regular IVIG replacement and antibiotic prophylaxis, alleviating their symptoms. Detailed case reports are provided in the Supplementary information.

To unveil the genetic etiology, WES was performed on P1 and P2. Based on the pedigree, an autosomal recessive mode of inheritance was assumed, and all rare nonsynonymous homozygous and compound heterozygous variants shared between the affected relatives were extracted. Further analysis of compound heterozygous variants shared in between the patients showed two missense variants within the *NFATC1* gene (ENST00000427363.7:c.1361C>T, p.S454L and ENST00000427363.7:c.2233G>A, p.V745M), segregating within the family members (Supplementary Figure 2A). The variant p.S454L lies in the region Rel homology domain (RHD) critical for DNA binding in the groove proximal to the AP- 1 binding site, while p.V745M is located in the transactivation domain B (TAD- B) on the C- terminal end of the protein (Figure 1C). No homozygous cases of these variants were reported in the gnomAD database and the frequency of observed heterozygous alleles are below 10^{-5} (last accessed 14.04.2023). Notably both amino acids at their particular position are conserved across species (Figure 1C). Although the variants in additional genes also segregated within the individuals, they were disregarded as being causative since they could not be related to the immunodeficiency status of the patients

(Supplementary Table 3).

Collectively, these data suggested that the compound heterozygous constellation in *NFATC1* has high probability for being disease-causing.

Identified *NFATc1* variants result in reduced protein stability, DNA binding, nuclear translocation and altered interaction with c- Jun

To elucidate the variants' pathogenic mechanisms, we tested their effect on the expression, localization and function of NFATc1. We first measured mRNA abundance and NFATc1 protein expression. Though mRNA levels were slightly higher, protein levels are comparable between patients and HC (Figure 1D and [Supplementary Figure 2B- C](#)) (P1 and P2, the patients whose material we had access to). We next assessed protein stability and found that ectopic expression of NFATc1^{S454L} and NFATc1^{V745M} variants exhibited reduced protein stability compared to NFATc1^{WT} in HEK cells (Figure 1E, [Supplementary Figure 2D- E](#)). Further, [we observed reduced NFATc1 nuclear translocation in stimulated T- lymphoblasts from patient 1 compared to HC \(Figure 1F and Supplementary Figure 3\)](#). Additionally, we detected a significant reduction in NFATc1 activation as per ELISA based DNA binding assay in patient T- cells compared to HC (Figure 1G). Given that TFs operate by interacting with multiple proteins on promoter sites of target genes, we studied the impact of the *NFATC1* variants on its interaction with the AP- 1 complex. Co- immunoprecipitation experiments demonstrated reduced interaction of both variants (more prominently in S454L) with c- Jun ([Supplementary Figure 4A](#)). Taken together, our data indicate that both *NFATC1* variants impact protein function through decreased stability, cellular mislocalization, reduced activation and aberrant interaction with c- Jun.

Dysfunctional NFATc1 impairs the differentiation, function, and survival of T cells

To systematically examine the effect of NFATc1 on lymphocyte differentiation, we performed detailed flow cytometric analysis on patients' PBMCs. T- , B- and NK- cell overall proportions remained unaltered throughout the disease course ([Supplementary Table 2, Supplementary Figure 4B- C](#)). Within the T- cell population, CD8⁺ T cells were increased resulting in a decreased CD4/CD8 ratio in all three patients ([Supplementary Table 2](#)). Despite absence of autoimmunity, we detected lower proportions of Treg- and Tfh- cells in patients (Figure 2A), consistent with *Nfatc1*- deficient murine models which

have aberrant Treg and T_H development and disproportional Th1, Th2 and Th17- populations¹². IFN- γ and IL- 4

productions were lower in CD4⁺CD45RA⁻ T cells in the patients, whereas the IL17 production was comparable with HCs (Supplementary Figure 4D). Similarly, CXCR3⁺CCR6⁻ populations were lower, as well as the GATA3 and T- Bet expression in Th2 (CCR4⁺CCR6⁻CXCR3⁻) and Th1(CCR4⁻CCR6⁻CXCR3⁺) enriched populations (Supplementary Figure 4E- F). Both CD4⁺ and CD8⁺ T- cell compartments contained lower naïve (CD45RA⁺) and central memory (TCM:CD45RA⁻CCR7⁺) with a corresponding increase in the effector memory (TEM:CD45RA⁻CCR7⁻) proportions (Figure 2B). Moreover, CD8⁺ T cells displayed reduced CD28 but enhanced CD57 expression, attesting to their chronic activation and exhausted phenotype (Figure 2C and Supplementary Figure 5). In summary, these results show that patients harboring *NFATC1* mutations exhibit altered proportions of T- helper lineage evidenced by reduced Tfh⁻, Treg⁻, Th1⁻ and Th2⁻ cells as well as aberrations in cytotoxic T- cells.

NFATc1 plays a prominent role in T- cell effector functions including cytokine productions (IL- 2, IFN- γ , TNF- α) and cytotoxicity^{9,10,13}. We therefore hypothesized that *NFATC1* LOF would compromise the effector responses of T- cells. Indeed, upon stimulation, patients' T- lymphoblasts exhibited diminished IL- 2 and IFN- γ production (Figure 2D) as well as reduced expression of CD107a indicating compromised lytic machinery (Supplementary Figure 6A). NFAT transcriptional control is essential for maintaining survival^{5,13- 15}, and indeed, patients' CD8⁺ T- lymphoblasts showed higher apoptosis compared to HCs, which could not be rescued by IL- 2 (Figure 2E). To exclude the possibility of an additional signaling defect that would impair T- cell functions, we tested the signaling cascades and Ca²⁺- flux following TCR stimulation. Except for a slight reduction of AKT phosphorylation, the downstream TCR responses (Ca²⁺- flux and ERK, p65, and S6 phosphorylation) remained intact (Supplementary Figure 6B- C), ruling out that additional defects proximal to NFAT signaling contribute meaningfully to cellular dysfunctions. Consistent with the role of *Nfatc1* in T- cell activation and proliferation in murine models^{16,17}, patient PBMCs showed defective proliferation and CD25 upregulation compared to HCs, predominantly in the CD8⁺ T- cell population (Figure 2F- G) and even more pronounced in the naïve T- cell compartment (Supplementary Figure 6D). Importantly, genetic reconstitution of wild- type *NFATC1* into patients' PBMCs restored both stimulation- induced CD25 expression and proliferation (Figure 2H- I) proving the pathogenicity of the patients' inherited *NFATC1* variants.

NFATc1 is required for survival and proliferation of activated mature B- cell populations

The Ca^{2+} /NFAT axis is critical for germinal center reactions, implicated in the regulation of ICOS and CD40L expression and thus, Tfh differentiation¹². Following TCR stimulation, there was reduced upregulation of CD40L in patient Tfh cells compared with the HCs (Supplementary Figure 6E). Despite normal absolute CD19⁺ B- cell numbers, we detected a phenotypic skewing of B- cell subsets with slightly lower switched- memory proportions and increased naïve B- cells in patients (Supplementary Figure 4C). These data are reminiscent of the mild effect on B- cell differentiation processes in the bone marrow and periphery of NFATc1- deficient murine models¹⁸. However, these mice have blunted proliferation and Ca^{2+} flux responses to stimulation, culminating in decreased immunoglobulin class switch and plasmablast formation, as well as aberrant cellular immune responses¹⁸. Therefore, we next assessed functional responses in patient B- cells. Compared with CD19⁺ B- cells from HC, patient cells were less responsive to stimulation with CD40L and IL4 as assessed by CD86 upregulation (Figure 2J). Notably, the activation marker CD25 was only partially upregulated in patient B- cells, suggesting impaired IL- 2- mediated survival and proliferation (Figure 2J). In response to CD40L and IL- 4/IL- 21 as well as CpG stimulations, patient B- cells were capable of class- switch recombination (CSR) to IgG *in vitro*, albeit with reduced frequency at day 7 (Supplementary Figure 7A), an effect likely due to impaired proliferative capacity which was lower following CpG exposure (Figure 2K). Given the reported Ca^{2+} flux perturbations in peripheral B- cells from NFATc1- deficient mice¹⁸, we tested Ca^{2+} dynamics in patient EBV B- cells. Patient derived EBV B- cells displayed reduced Ca^{2+} flux upon ionomycin treatment (Figure 2L), an effect that was rescued upon transfection with WT- *NFATc1* vector on P1 EBV B- cells (Supplementary Figure 7B). These data add corroborating evidence for the causality of the dysfunctional NFATc1 in patients leading to an impaired B- cell function. Taken together, these results suggest that intact NFATc1 is required to relay signals essential for survival and proliferation of activated mature B- cell populations.

Transcriptomic analysis of NFATc1 patients' lymphocytes indicates chronic inflammation and a tolerogenic/senescent signature

To better understand how NFATc1 dysfunction impacts the patients' lymphocytes, we compared the basal transcriptome and TCR repertoire of lymphocytes between P1 and P2 and HCs utilizing droplet based single- cell RNA sequencing (10x Genomics). The number

of TCR $\alpha\beta$ clonotypes in patients' T- cell populations, particularly within the CD8⁺- TEM fraction

(Supplementary Figure 8), were lower indicating a diminished TCR $\alpha\beta$ repertoire diversity (Figure 3A). Consistent with our FACS-based immunophenotyping (Figure 2B), transcriptional profiling confirmed reduced naïve CD4⁺ and CD8⁺ T cells with a concomitant skewing towards a TEM phenotype (Figure 3B- C), as well as reduced Tregs, and decreased CCR7 and IL7RA expression, similar to observations in NFATc1- deficient murine models¹⁰.

Differential gene expression analysis between the patients and controls on CD4⁺ and CD8⁺ T cells (Figure 3D) showed increased transcription of genes associated with chronic inflammation (*CD70*, *GPR65*, *JUNB*, *MAP3K8*)¹⁹, cellular stress (*MTRNRL2*, *SDF2L1*)²⁰⁻²² and tolerogenic signals (*LGALS1*, *CREM*, *AREG*, *NR4A2*)²³⁻²⁵. Consistently, an activated and terminally differentiated effector state (*PRDM1*)²⁶ was further evidenced by reduced *TCF7*, *LEF1* and *KLF7* expressions in the CD8⁺ compartment^{24,27,28}, altogether corroborating the molecular evidence for an anergic/exhausted state of patient T cells (Figure 3D). We performed a gene set enrichment analysis on 16 pre-defined pathways (Supplementary Table 8) and detected a significant enrichment in anergy/exhaustion pathway in the patients compared with HCs (hypergeometric test, FDR \leq 0.05)²⁹. We assessed the altered expression of selected marker genes at protein level (CD70, PRDM1) using flow cytometry (Supplementary Figure 9). We then focused on the expression profile within the CD8⁺- TEM compartment, constituting the largest CD8⁺ T- cell fraction having differential distribution among the controls and patients. Interestingly, within this population, we observed a significant increase in genes including *SGK1* and *PIM3* implicated in connecting T- cell fate determination to cellular metabolic signals such as environmental nutrient deprivation and/or mTOR activation^{30,31} (Figure 3E). Collectively, transcriptome profiling of the NFATc1- dysfunctional patients revealed a state of chronic activation, increased cellular stress response and anergy in T cells.

Within the B- cell compartment, differential gene expression analysis revealed 16 genes having altered expression levels in the patients compared with HCs. Interestingly, we detected reduced expression of several immunoglobulin heavy and light chain genes, including *IGHV5-10-1*, *IGHV1-24*, *IGHV1-26* and *IGLV1-47* (Figure 3F), similar to the NFATc1- deficient murine models, suggesting a role for NFATc1 as a facilitator of Ig gene locus accessibility³². Pathway analysis of up-regulated genes

confirmed the patients' proinflammatory state with a significant enrichment in TNF α /NF κ B signaling (Supplementary Table 9). Upregulation of genes such as *ZFP36L2*, *KLF3*, *PRDM4* and *ZBP1*, which are usually

expected to be downregulated during the transition from naïve to mature B- cells, suggested a differentiation defect. Consistently, we detected a reduced differentiation to plasmablasts (CD19⁺CD27⁺CD38⁺) upon stimulation with CD40L and IL- 4 or IL- 21 (Supplementary Figure 10).

Altered global chromatin landscape in human NFATc1 dysfunction

NFATc1 regulates chromatin remodeling and increases DNA accessibility to interacting TFs³³. Based on our earlier data showing reduced binding of NFATc1 to DNA and AP- 1 complex, we hypothesized reduced accessibility of NFAT mutants at the NFAT sites of *IL2* promoter. Thus, we performed an assay for transposase- accessible chromatin with high- throughput sequencing (ATAC- seq) on stimulated patient and HC T- lymphoblasts. Analysis of the consensus peaks at the promoter sites confirmed a decreased accessibility of the *IL2* promoter (Figure 4A) in patients, alongside other genes involved in T- cell proliferation and effector responses (*CCNA1*, *TESPA1*, *IL12RB2*, *CD44*, *PAK1*, *LEF1*) (Figure 4B). The motif heatmap (Figure 4C) shows z- scores of chromatin accessibility for the top 50 most significantly ($p_{adj} < 0.05$) variable motifs across samples. The majority of the FOS- JUN motifs have a reduced pattern of chromatin accessibility in the patients, as well as several other AP1 complex family members including BATF (Basic leucine zipper transcriptional factor ATF- like). AP- 1 transcription complex comprises numerous basic region- leucine zipper proteins that belong to different families (JUN, FOS, ATF, BATF and MAF) and form heterodimers to execute transcriptional activity. The members of this family such as BATF, might control other genes than the typical cJUN/cFOS heterodimers, or can replace those heterodimers under different physiological conditions^{34,35}. Collectively, ATACseq data suggest an overall reduced chromatin accessibility for AP1 complex motifs in the patient cells. Gene ontology (GO) term enrichment analysis of unique accessibility sites for patients and HCs revealed HC- specific GO enrichments of the genes involved in adaptive immune response, effector functions and activation responses implying reduced accessibility of corresponding sites in patient cells (Figure 4D). Altogether, these data support our earlier findings on reduced IL- 2 production caused by dysfunctional NFATc1 in patient T cells, with reduced accessibility of the chromatin regions required for T- cell activation.

NFATc1 dysfunction delays T- cell activation, which is associated with perturbed metabolic responses

To better understand the effect of NFATc1 deficiency on the temporal patterning of T- cell activation and proliferation responses, we performed detailed time- course experiments. Interestingly, determinants of activation and proliferation which were clearly different at earlier timepoints, were no longer distinguishable between patient and HC CD8⁺ T cells 7 days after stimulation (Figure 5A). As NFATc1 fine- tunes activation and senescence processes⁸ we assessed the expression profile of checkpoint inhibitors typically upregulated upon TCR activation in parallel to surface CD25. We observed a delayed upregulation of PD- 1, LAG3 and AITR/GITR upon TCR stimulation, particularly in patient CD8⁺ T cells in a trend reminiscent of the delayed activation (Figure 5B, Supplementary Figure 11A). A slight reduction in activation and proliferation was evident in CD4⁺ cells, albeit to a lesser extent than the CD8⁺ T cells, while exhaustion parameters were comparable (Supplementary Figure 11B). We hypothesized that the delay in activation is preceded by an altered transcriptional program in patient T cells. Thus, we stimulated PBMCs until day 3 which corresponded to the timepoint with the largest difference in proliferation between the patients and HCs, and performed bulk RNA sequencing on sorted CD8⁺ T cells. We analyzed enrichment of gene sets for 50 “hallmark” functions and pathways³⁶ through calculating normalized enrichment score (NES), which represents enrichment of genes from a tested gene set towards the top of the ranked list (positive NES) or the bottom of the ranked list (negative NES), respectively. In our dataset, it shows the gene enrichment profile of the stimulated T cells in comparison to unstimulated cells. TCR stimulation induced a global increase in the signals from pathways regulating cell cycle, ribosomal organization, protein translation and unfolded protein response, as well as metabolic signatures, including mTOR signaling in both HCs and patients (Figure 5C- D). In patients, a statistically significant positive enrichment is present for OXPHOS in the upregulated gene set upon stimulation compared to the unstimulated samples, whereas in HCs the contribution of oxidative pathway genes to the upregulated dataset is not significant. These data reveal a transcriptional disconnect between the expression profiles induced upon activation in HC compared to NFATc1 defective cells.

Given the impaired glycolysis in NFATc1- deficient murine models¹⁰, we next focused on

the genes regulating glycolysis (such as *HK2*, *ENO*, *PGK2*, *PFK2*) and observed a differentially

reduced expression pattern in patients compared to the HCs (Figure 5E). These data prompted us to analyze the metabolic parameters and functional capacity of patient T cells. We assessed glucose uptake in activated CD8⁺ T- lymphoblasts using the fluorescent glucose analogue 2- NBDG and observed that patients' cells took up less glucose compared with HCs, despite equivalent GLUT1 surface levels (Figure 6A and Supplementary Figure 12A- B). Next, we measured lower glycolytic rate and glycolytic reserve capacity in patients' CD8⁺ T- lymphoblasts upon stimulation compared to HC. Conversely, no major effect was observed on OXPHOS and mitochondrial respiration in patient' T- lymphoblasts (Figure 6B). These findings including reduced glucose uptake and glycolysis capacity due to an altered transcriptome, phenocopy those of CD8⁺ T cells from *Nfatc1*^{-/-} mice¹⁰. Consistent with hexokinase 2 (HK2), a glycolytic marker, expression being regulated by NFATc1¹⁰, we observed that the stimulation- induced increase in HK2 expression was almost absent in P1 and reduced in P2 T- lymphoblasts, whereas expression of GLUT3, one of the major glucose transporter in addition to GLUT1³⁷ remained unaltered (Figure 6C- D and Supplementary Figure 12- 13). Accordingly, LC- MS metabolomics analysis revealed higher hexose (representing glucose) and pentose levels with a concomitant decrease in downstream glycolytic metabolites in patient T- cells, consistent with an obstructed initial step of glycolysis (Figure 6E).

NFATc1- mutant T cells compensate for impaired glycolysis by enhancing lipid metabolism

The observation that the delayed patient T- cell activation and proliferation responses could “catch- up” prompted us to evaluate whether NFATc1- dysfunctional cells were adapting by increasing their reliance on alternative metabolic substrates. Not only was the expression of CPT1a, a transporter of FAs into the mitochondria and key regulator of FA metabolism, higher in stimulated patient T cells (Figure 6C- D, Supplementary Figure 13), but lipid uptake determined using Bodipy FL C16 was higher in patients' T- lymphoblasts both with, and without stimulation compared to HCs (Figure 7A, Supplementary Figure 14A). Interestingly, lipidomic analysis revealed that although overall lipid populations increased with stimulation in both HC and patients (Figure 7B), consistent with the stimulation induced increased in lipid uptake seen with Bodipy (Figure 7A). The extent of the increase in the triacylglycerol pool is markedly attenuated in

patient cells compared with HC (Figure 7C- D). Together, these data suggest that patient cells had a shifted substrate preference towards FAO. Indeed,

fluxomics experiments utilizing [$^{13}\text{C}_{16}$]- palmitic acid revealed patients' T lymphoblasts to have higher tracer incorporation into citrate isotopologues, indicating enhanced flux of exogenously administered, palmitate- derived carbons into the TCA cycle (Figure 7E). Considering the exhausted phenotype of the patient cells and heterogeneity in the T- cell pool, we sought for innovative ways to delineate, at the T- cell subpopulation level, the consequences of the *NFATC1* mutations on metabolic responses. We utilized the recently described flow cytometry- based metabolic profiling technique SCENITH and extended our understanding at the single- cell level³⁸. While patients' CD4^+ T cells displayed similar metabolic trends compared with HC (Supplementary Figure 14B), consistent with the impaired glycolytic capacity observed in patient T- lymphoblasts during the glycolysis stress test (Figure 6B), further analysis of the CD8^+ T- cell subpopulation revealed that the effector memory ($\text{CD45RA}^-\text{CCR7}^+$) population was most different compared with HC (Figure 7F) and thus, most sensitive to NFATc1 deficiency. Taken together, these data strongly argue that *NFATC1* mutations impair glycolysis in CD8^+ T cells which is associated with delayed CD8 T- cell effector responses and a metabolic shift towards β - oxidation and FA utilization.

Pharmacological modeling of patient phenotype in primary T cells recapitulates the metabolic flexibility observed in patient cells

To better understand the molecular association between the impaired glycolysis in the NFATc1- dysfunctional patient cells and the adaptation towards FAO, we aimed to model the patient phenotype pharmacologically using lymphocytes derived only from HCs. Consistent with established literature, inhibiting glycolysis in HC PBMCs using 2- Deoxyglucose (2- DG) reduced activation and proliferation^{1,2}. In contrast to NFATc1- deficient mice data¹⁰, such defects in activation and proliferation, secondary to ablated glycolysis, could not be rescued with IL- 2 treatment (Supplementary Figure 14C- D). Next, we assessed the effect of 2- DG on IL- 2 production of the HC- lymphoblasts. Lower IL- 2 production upon 2- DG- treatment further corroborated the necessity of glycolysis for appropriate effector responses (Supplementary Figure 14E). To rule out that the defects in activation and proliferation responses in patient PBMCs merely reflected differences in T- cells subset proportions, we performed time course experiments in sorted HC naïve T- cells treated with Cyclosporin- A³⁹ to model NFAT inhibition, or

2- DG to inhibit glycolysis, and measured their functional and metabolic responses. In a pattern reminiscent of the patients, stimulated CD8⁺ T cells exposed to 2- DG,

whilst delayed initially with respect to the proliferation and activation (Figure 7G), managed to match responses of the stimulated, vehicle- treated cells by day 8. Importantly, this recovery in functional responses after the initial delay in 2- DG- treated cells was associated with a concomitant increase in lipid uptake (Figure 7G). Additionally, HK2 upregulation upon stimulation was normal in 2- DG group whereas it was reduced in CsA treated cells (Figure 7H), consistent with our patient data. Furthermore, both CsA and 2- DG treatment promoted [¹³C₁₆]- palmitic acid incorporation into TCA cycle metabolites following TCR stimulation compared with stimulated, vehicle- treated control cells (Figure 7I). These data strongly suggest that glycolysis inhibition is sufficient to induce metabolic adaptations towards FAO. NFATc1- mutant CD8⁺ T cells possess a “delayed but not absent” responsiveness to stimulation, possibly associated with a subsequent adaptation towards FA utilization. We next tested whether CD8⁺ T- cell effector functions could be improved through therapeutic metabolic reprogramming. We reasoned that early priming of cells towards FAO might diminish the delay in functional responses, in CD8⁺ T cells with ineffective glycolysis. We primed patient CD8⁺ T cells with metformin and rosiglitazone, two therapies well- documented for their effects on lipid catabolism⁴⁰. Not only did CD8⁺ T- lymphoblasts from both patients increase IL- 2 production with their treatment (Supplementary Figure 14F), but treatment of patient PBMCs with metformin and rosiglitazone simultaneously with stimulation led to improved proliferation, predominantly in rosiglitazone- treated patient CD8⁺ T cells (Supplementary Figure 14G- H). Taken together, these results demonstrate that NFATc1- mutant T cells may adapt to restricted glycolysis likely by shifting their substrate preference towards FAO following stimulation thereby retaining some degree of functional capacity, which might be enhanced by metabolic priming as a potential therapeutic modulation.

Discussion

Here, we describe patients with inherited mutations in *NFATc1* that present with a novel combined immunodeficiency characterized by recurrent viral and bacterial infections, due to impaired T- and B- cell activation and proliferation. Through a detailed profiling of the patient's immunophenotype and comprehensive molecular experiments, we further authenticate the involvement of NFATc1 in establishing a cellular milieu that permits optimum glycolytic responses in T cells and reveal evidence of metabolic plasticity in the context of impaired glycolysis observed in patient T cells to remedy delayed effector responses. Lastly, through metabolic priming of patient T cells, we provide preliminary proof- of- concept pre- clinical evidence for the therapeutic improvement of genetically defective T cells.

The role of NFAT family of transcription factors, including the contribution of SOCE to the regulation of NFAT axis on different phenotypes has been extensively characterized in mouse models. Recently, patients with LOF *NFATC2* were reported and characterized by joint contractures, osteochondromas, and recurrent B- cell lymphoma⁴¹. Aspects of our patients' clinical presentations are shared by patients with NFATc2 deficiency including the aberrant T- cell functions. However, skeletal manifestations appear somewhat divergent. While NFATC1- mutated patients (P1 and P2) presented with scoliosis, likely reflecting an imbalance in bone remodeling processes for which NFATc1 has a well- documented role⁴², the joint contractures observed in the NFATC2- mutated patients points towards the cartilage as the origin of the skeletal phenotype. A possible explanation for this is the expression profile differences between these proteins with NFATC2 being more widely expressed compared with NFATC1 whose expression is more limited to the lymphoid/bone marrow compartment.

The phenotype of our patients is also reminiscent of ORAI/STIM1 deficiencies, the prototype diseases of defective SOCE⁶, who present with normal lymphocyte numbers, despite impairments in their activation and proliferation responses. Defective T- and B- cell activation in ORAI/STIM1 deficiency manifests as blunted NFAT activation and downstream effects on cytokine production⁶. Murine models revealed the essential role of NFATc1 in the regulation of multiple steps of both B and T- cell development^{5,10,13,18,32}. The defects in B- cell differentiation, activation and class switch functions in our patients are consistent with mouse models where a prevailing theory suggests a threshold level of

NFATc1 expression is

necessary for proper B- cell development. **The relatively milder phenotype observed in patient 2 might be due to the higher protein expression.** However, larger cohorts of NFATc1- defective patients will be required to address such a relationship between NFATc1 protein expression and severity of clinical presentations and/or impaired B- cell functioning. SOCE also controls transcriptional networks that determine the differentiation of CD4⁺ T cells into T_H and T_{reg}, evidenced by STIM1- deficient patients developing autoimmune thrombocytopenia and hemolytic anemia. While autoimmunity is also a defining feature in *Nfatc1*^{-/-} mice, no such clinical evidence for autoimmunity in our patients was observed despite having fewer circulating T_{reg}- cells. Nonetheless, further patient cohorts will be needed to clarify whether any causal link between NFATc1 dysfunction and autoimmunity exists.

Despite the substantial data generated using murine models, mechanisms by which NFAT controls the switch of T- cells from the quiescent to proliferative state have remained elusive. A proposed mechanism involves transcriptional regulation of *IL2*^{43,44}, however, results from animal studies remain discordant^{7,37}. Although in some animal studies, IL- 2 partially rescued the T- cell dysfunction¹⁰, additional IL- 2 did not rescue apoptosis in our patient cells and only slightly improved TCR- induced proliferation in ORAI/STIM1- deficient patients³⁷. Our finding of impaired glycolytic capacity in NFATC1 mutant T- cells is consistent with *Nfatc1* and *Stim1* deficient murine T- cells^{10,34} attesting to the essential role of the SOCE/NFAT axis in regulating glycolytic capacity and subsequent T- cell proliferation. However, that functional responses were delayed rather than absent in the NFATC1 mutant T- cells, prompted us to question whether this delay corresponded to cells adapting to the impaired glycolytic capacity by enhancing alternative metabolic preferences. Indeed, fluxomics experiments confirmed palmitate- derived carbons were incorporated more readily into the TCA cycle in NFATC1 mutant lymphocytes suggesting an increased utilization on FAO⁴⁵.

As the initial engagement of glycolysis appears most relevant in naïve cells in terms of coordinating initial effector responses^{1,2}, we assessed whether naïve CD8⁺ T- cells would similarly modify their metabolic preference towards FAO upon the inhibition of glycolysis induced with the use of 2- DG. 2- DG inhibited initial proliferation and activation responses in naïve CD8⁺ T- cells from HCs consistent with reported literature^{1,2} and mirrored the delayed effector responses in our patient T- cells. Similar to our patient cells,

TCA cycle incorporation of ^{13}C -labeled palmitate-derived carbons were higher in TCR-activated T-cells exposed to 2-

DG compared with vehicle, indicating a greater reliance on FAs as a substrate. Importantly, markers of increased lipid uptake and incorporation into the TCA cycle induced by 2- DG preceded the recovery of functional responses to levels of the vehicle- treated cells. Thus, while observations that proliferation and survival of T- cells can persist *in vitro* when glycolysis is ablated have been reported⁴⁵, to the best of our knowledge, this is the first evidence of metabolic adaptation established in the setting of an IEI.

Not addressed specifically in this study are the underlying stimuli and mechanisms for the shifted preference toward FAO in NFATC1 mutant T cells. Thus, while *NFATC1* mutant T cells have altered HK2 expression following stimulation, whether this is responsible for the glycolytic defect in patient T- cells is uncertain, particularly given the data from murine *HK2*^{-/-} T- cells which retain intact glycolysis and are grossly immunologically normal⁴⁶. Kaymak et al⁴⁷ revealed that shifted fuel preferences in T cells could occur in the absence of major differences in global transcriptional changes of metabolic programs⁴⁷ suggesting that metabolite concentrations *per se* exert a greater influence on the immediate and dynamic control of metabolic fuel selection⁴⁸. We focused our attention on lipids for which associated metabolic pathways are sensitive to changes in glucose utilization dynamics^{49- 51}. NFATc1 defective T- cells had attenuated increase in TAG pool following stimulation, despite markers of FA uptake being higher suggests increased utilization, consistent with the elevated CPT1a levels and palmitate- derived carbon incorporation into the TCA cycle. However, whether increased FAO is engaged to alleviate an energetic deficit or for some other compensation is unknown. The pentose phosphate pathway(PPP) is essential for T- cell functions, particularly for proliferative purposes where glucose gets consumed to generate biosynthetic precursors for DNA and RNA synthesis as well as NADPH which is required for *de novo* FA and cholesterol biosynthesis⁵². Thus, it is possible that FAO is engaged in response to impaired glucose- PPP flux in order to sustain cytosolic NADPH pools^{51,53}. Inadvertently, such an adaptation would serve not only to sustain proliferative capacity, but also act to promote survival by supporting defenses against oxidative stress^{51,53- 55}. Additional advanced substrate- tracing experiments would be required to evaluate cross- metabolic pathway regulation and engagement as well as shifted utilization of other non- conventional substrates such as amino acids and lactate by NFATc1 mutant T- cells.

Our observations that contribution of FA to oxidative metabolism is higher in NFATc1- mutant T- cells and that 2- DG treatment promotes a metabolic shift towards FA utilization, led us to consider therapeutic priming of patient T- cells in order to promote FAO and evaluate whether this might improve T- effector cell functionality. We tested this hypothesis using metformin and rosiglitazone; two drugs with well- characterized effects on FAO^{56- 59}. These drugs were able to induce a modest, albeit reproducible increase in IL- 2 expression in patient T lymphocytes expanded *in vitro*. Experiments performed on limited patient material restricted us from making firm conclusions about these data regarding their significance or clinical relevance and obtaining *in vivo* evidence from patients e.g. in the scope of a clinical trial are outside the scope of the current study. Nonetheless, a growing body of literature supports the premise that increasing FAO can improve the development and quality of CD8⁺ T cells⁵² suggesting metabolic priming as a promising line of inquiry. Additional experiments are required to elucidate how IL- 2 production is improved by these compounds in the NFATc1- defective T cells. It would also be interesting to assess whether murine *Nfatc1*^{-/-} T cells similarly adapt to restricted glycolysis by increasing FA utilization and whether their immune- dysregulated features can be improved with pharmacological approaches that target metabolic pathways and to dissect the responsible underlying cellular mechanisms.

Collectively, we report *NFATC1*- deficiency as a novel IEI and provide evidence that NFATC1 mutant T- cells adapt to impairments in their glycolytic capacity by increasing their reliance on FA utilization showcasing the phenomena of metabolic plasticity in a transcriptionally defective genetic landscape. The extent to which other IEIs can be classified by specific metabolic signatures irrespective of their genetic etiology and/or sensitivity to therapies targeting metabolic pathways warrants further research.

Acknowledgements: We thank the patients and their family members for their participation in our study. We also thank the Biomedical Sequencing Facility (BSF) for their WES, RNA- seq and ATACseq service and Bergthaler lab for the use of Seahorse XFe 96 machine at the CeMM Research Center of Molecular Medicine (CeMM) of the Austrian Academy of Sciences. We thank Daniela Reil and the Molecular Discovery Platform at CeMM for technical support with metabolomics analyses. We thank MUW Core Facility Flow Cytometry Unit and Andreas Spittler for their help in imaging flow cytometry. We would like to thank Wolfgang Weninger for providing the infrastructure required for processing the single cell RNA- sequencing libraries and relevant discussions. **Funding:** This study has been supported by the European Research Council Consolidator Grant iDysChart (ERC grant agreement number: 820074) (to K.B.), SB has been supported by The Scientific and Technological Research Council of Turkey (318S202). M.J.K has been supported by an FWF Lise Meitner Postdoctoral Fellowship. J.B has been supported by a DOC Fellowship of the Austrian Academy of Sciences (No 5590). CvW has been supported by a Postdoctoral Fellowship of the P.T. Engelhorn Foundation. B.R. has been supported by a FFG Industry Grant. **Author contributions:** S.K.B. performed most of the experiments on patient material, analyzed and interpreted the patient and experimental data. S.K.B., S.G, J.B. and T.S., performed the biochemical experiments, with help from VH. S.K.B. supervised S.G. M.K. and S.K.B. planned the metabolism experiments, performed and analyzed them together, with technical assistance of S.G. M.S. analyzed the RNA- seq data under supervision of C.B. P.R. analyzed the RNAseq and ATACseq data. CH analyzed the scRNA- seq data and rerun the pipeline for the ATACseq under the supervision of F.H. R.J.H. identified the variant, run the WES, ATACseq and RNA- seq prep; A.F. performed the segregation analysis and protein conservation analysis, and qPCR experiments. I.C. and M.V. gave intellectual input. J.B. assisted in imaging analysis and provided critical intellectual input. S.K.B. and B.R. prepared samples and interpreted the scRNA- seq results together. B.R. performed the B- cell activation, proliferation and class switch experiments. Y.M. assisted in tissue culture of T cells and performing imaging experiments. CvdW run WB for co- Ip experiments, assisted in the data analysis of hexokinase assay, provided intellectual input and controlled manuscript. S.Z. assisted in tissue culture of B cells and transfection of EBV B- cells. M.T. assisted in the B cell class switch assays. **A.B. reran the pipeline for RNAseq experiments and replotted the GSEA**

graphs. L.E.S. performed scRNA sequencing under the supervision of M.F. S.B. recruited the

patients in Turkey supervised the patient follow-ups, N.K., R.B., S.B.E., E.K., A.O. followed the patients and assisted in the collection of medical data. R.A. provided the necessary material, protocol and consultancy for SCENITH experiments. L.D. provided protocols and consultancy for the T cell functional experiments (T-cell expansion, imaging and degranulation). T.H. ran the MS for metabolomics, lipidomics and fluxomics and made the initial data analysis. S.K.B., M.K., I.C.O. and K.B. wrote the manuscript with input from all co-authors. K.B. conceptualized and coordinated the study, provided laboratory resources, and took overall responsibility of the study. **Competing interests:** The authors declare no competing financial interests. **Data and materials availability:** Processed single-cell RNA-seq data are going to be openly available via Gene Expression Omnibus (GEO, accession number pending). Raw sequencing reads are going to be available under controlled access via the European Genome-Phenome Archive (EGA, accession number pending) to safeguard patient privacy. R code used for the analysis for single-cell RNA-seq data are going to be available via GitHub: <https://github.com/cancerbits/nfatc1>. Raw data from LC-MS will be available in Massive (identifier number pending).

REFERENCES

1. Geltink RIK, Kyle RL, Pearce EL. Unraveling the Complex Interplay Between T Cell Metabolism and Function. *Annu Rev of Immunol.* Apr 26 2018;36:461- 488. doi:10.1146/annurev- immunol-042617- 053019
2. Buck MD, Sowell RT, Kaech SM, Pearce EL. Metabolic Instruction of Immunity. *Cell.* May 4 2017 ;169(4):570- 586. doi:10.1016/j.cell.2017.04.004
3. Hermann- Kleiter N, Baier G. NFAT pulls the strings during CD4+ T helper cell effector functions. *Blood.* Apr 15 2010;115(15):2989- 97. doi:10.1182/blood- 2009- 10- 233585
4. Hogan PG. Calcium- NFAT transcriptional signalling in T cell activation and T cell exhaustion. *Cell Calcium.* May 2017;63:66- 69. doi:10.1016/j.ceca.2017.01.014
5. Vaeth M, Feske S. NFAT control of immune function: New Frontiers for an Abiding Trooper. *F1000Res.* 2018;7:260. doi:10.12688/f1000research.13426.1
6. Lacruz RS, Feske S. Diseases caused by mutations in ORAI1 and STIM1. *Ann N Y Acad Sci.* Nov 2015;1356(1):45- 79. doi:10.1111/nyas.12938
7. Vaeth M, Kahlfuss S, Feske S. CRAC Channels and Calcium Signaling in T Cell- Mediated Immunity. *Trends Immunol.* Oct 2020;41(10):878- 901. doi:10.1016/j.it.2020.06.012
8. Martinez GJ, Pereira RM, Aijo T, et al. The transcription factor NFAT promotes exhaustion of activated CD8(+) T cells. *Immunity.* Feb 17 2015;42(2):265- 278. doi:10.1016/j.immuni.2015.01.006
9. Baur J, Otto C, Steger U, et al. The Transcription Factor NFATc1 Supports the Rejection of Heterotopic Heart Allografts. *Front Immunol.* 2018;9:1338. doi:10.3389/fimmu.2018.01338
10. Klein- Hessling S, Muhammad K, Klein M, et al. NFATc1 controls the cytotoxicity of CD8(+) T cells. *Nat Commun.* Sep 11 2017;8(1):511. doi:10.1038/s41467- 017- 00612- 6
11. Shahin T, Kuehn HS, Shoeb MR, et al. Germline biallelic mutation affecting the transcription factor Helios causes pleiotropic defects of immunity. *Sci Immunol.* Nov 26 2021;6(65):eabe3981. doi:10.1126/sciimmunol.abe3981
12. Martinez GJ, Hu JK, Pereira RM, et al. Cutting Edge: NFAT Transcription Factors Promote the Generation of Follicular Helper T Cells in Response to Acute Viral Infection. *J Immunol.* Mar 1 2016;196(5):2015- 9. doi:10.4049/jimmunol.1501841
13. Klein- Hessling S, Rudolf R, Muhammad K, et al. A threshold level of NFATc1 activity facilitates thymocyte differentiation and opposes notch- driven leukaemia development. *Nat Commun.* Jun 17 2016;7:11841. doi:10.1038/ncomms11841
14. Rudolf R, Busch R, Patra AK, et al. Architecture and expression of the nfatc1 gene in lymphocytes. *Front Immunol.* 2014;5:21. doi:10.3389/fimmu.2014.00021
15. Yoshida H, Nishina H, Takimoto H, et al. The transcription factor NF- ATc1 regulates lymphocyte proliferation and Th2 cytokine production. *Immunity.* Jan 1998;8(1):115- 24. doi:10.1016/s1074- 7613(00)80464- 1
16. Pachulec E, Neitzke- Montinelli V, Viola JP. NFAT2 Regulates Generation of Innate- Like CD8(+) T Lymphocytes and CD8(+) T Lymphocytes Responses. *Front Immunol.* 2016;7:411. doi:10.3389/fimmu.2016.00411
17. Guram K, Kim SS, Wu V, et al. A Threshold Model for T- Cell Activation in the Era of Checkpoint Blockade Immunotherapy. *Front Immunol.* 2019;10:491. doi:10.3389/fimmu.2019.00491
18. Bhattacharyya S, Deb J, Patra AK, et al. NFATc1 affects mouse splenic B cell function by controlling the calcineurin- - NFAT signaling network. *J Exp Med.* Apr 11 2011;208(4):823- 39. doi:10.1084/jem.20100945
19. Huang XP, Karpiak J, Kroeze WK, et al. Allosteric ligands for the pharmacologically dark receptors GPR68 and GPR65. *Nature.* Nov 26 2015;527(7579):477- 83. doi:10.1038/nature15699
20. Mehta HH, Xiao J, Ramirez R, et al. Metabolomic profile of diet- induced obesity mice in response to humanin and small humanin- like peptide 2 treatment. *Metabolomics.* Jun 6 2019;15(6):88. doi:10.1007/s11306- 019- 1549- 7
21. Sasako T, Ohsugi M, Kubota N, et al. Hepatic Sdf2l1 controls feeding- induced ER stress

and regulates metabolism. *Nat Commun.* Feb 27 2019;10(1):947.
doi:10.1038/s41467-019-08591-6

22. Yen K, Lee C, Mehta H, Cohen P. The emerging role of the mitochondrial- derived peptide humanin in stress resistance. *J Mol Endocrinol.* Feb 2013;50(1):R11- 9. doi:10.1530/JME- 12- 0203
23. Femel J, van Hooren L, Herre M, et al. Vaccination against galectin- 1 promotes cytotoxic T- cell infiltration in melanoma and reduces tumor burden. *Cancer Immunol Immunother.* Jan 11 2022;doi:10.1007/s00262- 021- 03139- 4
24. Seo W, Jerin C, Nishikawa H. Transcriptional regulatory network for the establishment of CD8(+) T cell exhaustion. *Exp Mol Med.* Feb 2021;53(2):202- 209. doi:10.1038/s12276- 021- 00568- 0
25. Zaiss DM, van Loosdregt J, Gorlani A, et al. Amphiregulin enhances regulatory T cell-suppressive function via the epidermal growth factor receptor. *Immunity.* Feb 21 2013;38(2):275- 84. doi:10.1016/j.immuni.2012.09.023
26. Kallies A, Hawkins ED, Belz GT, et al. Transcriptional repressor Blimp- 1 is essential for T cell homeostasis and self- tolerance. *Nat Immunol.* May 2006;7(5):466- 74. doi:10.1038/ni1321
27. Raghu D, Xue HH, Mielke LA. Control of Lymphocyte Fate, Infection, and Tumor Immunity by TCF- 1. *Trends Immunol.* Dec 2019;40(12):1149- 1162. doi:10.1016/j.it.2019.10.006
28. Seo H, Chen J, Gonzalez- Avalos E, et al. TOX and TOX2 transcription factors cooperate with NR4A transcription factors to impose CD8(+) T cell exhaustion. *Proc Natl Acad Sci U S A.* Jun 18 2019;116(25):12410- 12415. doi:10.1073/pnas.1905675116
29. Federico A, Monti S. hypeR: an R package for geneset enrichment workflows. *Bioinformatics.* Feb 15 2020;36(4):1307- 1308. doi:10.1093/bioinformatics/btz700
30. Heikamp EB, Patel CH, Collins S, et al. The AGC kinase SGK1 regulates TH1 and TH2 differentiation downstream of the mTORC2 complex. *Nat Immunol.* May 2014;15(5):457- 64. doi:10.1038/ni.2867
31. Liu Z, Han M, Ding K, Fu R. The role of Pim kinase in immunomodulation. *Am J Cancer Res.* 2020;10(12):4085- 4097.
32. Giampaolo S, Wojcik G, Klein- Hessling S, Serfling E, Patra AK. B cell development is critically dependent on NFATc1 activity. *Cell Mol Immunol.* May 2019;16(5):508- 520. doi:10.1038/s41423- 018- 0052- 9
33. Pham LV, Tamayo AT, Li C, Bueso- Ramos C, Ford RJ. An epigenetic chromatin remodeling role for NFATc1 in transcriptional regulation of growth and survival genes in diffuse large B- cell lymphomas. *Blood.* Nov 11 2010;116(19):3899- 906. doi:10.1182/blood- 2009- 12- 257378
34. Miller M. The importance of being flexible: the case of basic region leucine zipper transcriptional regulators. *Curr Protein Pept Sci.* Jun 2009;10(3):244- 69. doi:10.2174/138920309788452164
35. Schraml BU, Hildner K, Ise W, et al. The AP- 1 transcription factor Batf controls T(H)17 differentiation. *Nature.* Jul 16 2009;460(7253):405- 9. doi:10.1038/nature08114
36. Subramanian A, Tamayo P, Mootha VK, et al. Gene set enrichment analysis: a knowledge- based approach for interpreting genome- wide expression profiles. *Proc Natl Acad Sci U S A.* Oct 25 2005;102(43):15545- 50. doi:10.1073/pnas.0506580102
37. Vaeth M, Maus M, Klein- Hessling S, et al. Store- Operated Ca(2+) Entry Controls Clonal Expansion of T Cells through Metabolic Reprogramming. *Immunity.* Oct 17 2017;47(4):664- 679 e6. doi:10.1016/j.immuni.2017.09.003
38. Arguello RJ, Combes AJ, Char R, et al. SCENITH: A Flow Cytometry- Based Method to Functionally Profile Energy Metabolism with Single- Cell Resolution. *Cell Metab.* Dec 1 2020;32(6):1063- 1075 e7. doi:10.1016/j.cmet.2020.11.007
39. Wong GK, Goldacker S, Winterhalter C, et al. Outcomes of splenectomy in patients with common variable immunodeficiency (CVID): a survey of 45 patients. Research Support, Non- U.S. Gov't. *Clin Exp Immunol.* Apr 2013;172(1):63- 72. doi:10.1111/cei.12039
40. Palsson- McDermott EM, O'Neill LAJ. Targeting immunometabolism as an anti- inflammatory strategy. *Cell Res.* Apr 2020;30(4):300- 314. doi:10.1038/s41422- 020- 0291- z
41. Sharma M, Fu MP, Lu HY, et al. Human complete NFAT1 deficiency causes a triad of joint

contractures, osteochondromas, and B- cell malignancy. *Blood.* Oct 27
2022;140(17):1858- 1874. doi:10.1182/blood.2022015674

42. Sitara D, Aliprantis AO. Transcriptional regulation of bone and joint remodeling by NFAT. *Immunol Rev.* Jan 2010;233(1):286- 300. doi:10.1111/j.0105- 2896.2009.00849.x
43. Nadeau S, Martins GA. Conserved and Unique Functions of Blimp1 in Immune Cells. *Front Immunol.* 2021;12:805260. doi:10.3389/fimmu.2021.805260
44. Xiao Y, Qureischi M, Dietz L, et al. Lack of NFATc1 SUMOylation prevents autoimmunity and alloreactivity. *J Exp Med.* Jan 4 2021;218(1)doi:10.1084/jem.20181853
45. Chang CH, Curtis JD, Maggi LB, Jr., et al. Posttranscriptional control of T cell effector function by aerobic glycolysis. *Cell.* Jun 6 2013;153(6):1239- 51. doi:10.1016/j.cell.2013.05.016
46. Mehta MM, Weinberg SE, Steinert EM, et al. Hexokinase 2 is dispensable for T cell-dependent immunity. *Cancer Metab.* 2018;6:10. doi:10.1186/s40170- 018- 0184- 5
47. Kaymak I, Luda KM, Duimstra LR, et al. Carbon source availability drives nutrient utilization in CD8(+) T cells. *Cell Metab.* Sep 6 2022;34(9):1298- 1311 e6. doi:10.1016/j.cmet.2022.07.012
48. Hackett SR, Zanutelli VR, Xu W, et al. Systems- level analysis of mechanisms regulating yeast metabolic flux. *Science.* Oct 28 2016;354(6311)doi:10.1126/science.aaf2786
49. Pearce EL, Walsh MC, Cejas PJ, et al. Enhancing CD8 T- cell memory by modulating fatty acid metabolism. *Nature.* Jul 2 2009;460(7251):103- 7. doi:10.1038/nature08097
50. Raud B, McGuire PJ, Jones RG, Sparwasser T, Berod L. Fatty acid metabolism in CD8(+) T cell memory: Challenging current concepts. *Immunol Rev.* May 2018;283(1):213- 231. doi:10.1111/imr.12655
51. Jeon SM, Chandel NS, Hay N. AMPK regulates NADPH homeostasis to promote tumour cell survival during energy stress. *Nature.* May 9 2012;485(7400):661- 5. doi:10.1038/nature11066
52. Klein Geltink RI, Edwards- Hicks J, Apostolova P, et al. Metabolic conditioning of CD8(+) effector T cells for adoptive cell therapy. *Nat Metab.* Aug 2020;2(8):703- 716. doi:10.1038/s42255- 020- 0256- z
53. Carracedo A, Cantley LC, Pandolfi PP. Cancer metabolism: fatty acid oxidation in the limelight. *Nat Rev Cancer.* Apr 2013;13(4):227- 32. doi:10.1038/nrc3483
54. Carracedo A, Weiss D, Leliaert AK, et al. A metabolic prosurvival role for PML in breast cancer. *J Clin Invest.* Sep 2012;122(9):3088- 100. doi:10.1172/JCI62129
55. Samudio I, Harmancey R, Fiegl M, et al. Pharmacologic inhibition of fatty acid oxidation sensitizes human leukemia cells to apoptosis induction. *J Clin Invest.* Jan 2010;120(1):142- 56. doi:10.1172/JCI38942
56. Nicoli F, Cabral- Piccin MP, Papagno L, et al. Altered Basal Lipid Metabolism Underlies the Functional Impairment of Naive CD8(+) T Cells in Elderly Humans. *J Immunol.* Feb 1 2022;208(3):562- 570. doi:10.4049/jimmunol.2100194
57. Xu L, Ma X, Verma N, et al. PPARgamma agonists delay age- associated metabolic disease and extend longevity. *Aging Cell.* Nov 2020;19(11):e13267. doi:10.1111/ace1.13267
58. Renner K, Geiselhoringer AL, Fante M, et al. Metabolic plasticity of human T cells: Preserved cytokine production under glucose deprivation or mitochondrial restriction, but 2- deoxy- glucose affects effector functions. *Eur J Immunol.* Sep 2015;45(9):2504- 16. doi:10.1002/eji.201545473
59. Zhou J, Massey S, Story D, Li L. Metformin: An Old Drug with New Applications. *Int J Mol Sci.* Sep 21 2018;19(10)doi:10.3390/ijms19102863
60. Hao Y, Hao S, Andersen- Nissen E, et al. Integrated analysis of multimodal single- cell data. *Cell.* Jun 24 2021;184(13):3573- 3587 e29. doi:10.1016/j.cell.2021.04.048
61. Love MI, Huber W, Anders S. Moderated estimation of fold change and dispersion for RNA- seq data with DESeq2. *Genome Biol.* 2014;15(12):550. doi:10.1186/s13059- 014- 0550- 8

Figure Legends

Figure 1. Identification of human NFATc1 mutations and molecular analysis of the impact of identified variants on protein stability, localization, function and interactions. (A)

Pedigree of multigenerational family; shaded symbols, affected patients having compound heterozygous variants in *NFATC1*; open symbols, healthy heterozygous carriers and wild- type subjects. Double lines indicate consanguinity. Crossed symbols designate deceased individuals. The genotype of the patients and family members is indicated below each symbol. The asterisk represents those individuals who underwent WES. (B) Chest X Ray and Thoracolumbal X- Ray showing scoliosis in P1 and P2 respectively (red arrows). (C) Illustration of the NFATc1 protein, with N- terminal regulatory domain, Rel homology domain (RHD) for DNA binding to the consensus sequence, and C- terminal transactivation domain (TAD- B). Location of variants are shown together with their conservation across several species. An

*(asterisk) means fully conserved, a : (colon) highly conserved and a . (period) weakly conserved residues. (D) Immunoblot showing NFATc1 expression in T cells from P1 and P2 (the patients whose material we could access) and healthy controls (HC). (E) Representative blot for protein stability analysis using cycloheximide (CHX) chase assay on HEK cells transfected with either empty vector, or Strep- HA- NFATc1^{WT}, - NFATc1^{S454L}, - NFATc1^{V745M}, or - NFATc1^{V745M+s454L} plasmids followed by 6 and 10 hours of cycloheximide treatment. Quantifications of NFATc1 expression from blots represented in (D) and (E) are provided in Supplementary Figure 2B, E. Quantification of similarity scores of nuclear translocation analysis of NFATc1 on (F) Representative images acquired with 60x magnification with Image Flow Cytometer (AMNIS[®]) (left) and similarity score quantification using IDEAS software (right) of NFATc1 nuclear translocation in feeder- expanded T- lymphoblasts from patients or HC, either unstimulated (unstim) or upon stimulation with soluble anti- CD3/CD28 antibodies (stim). Data show significant nuclear translocation in HC cells upon stimulation and no or slight nuclear translocation in T cells from patients 1 and 2, respectively. Representative images for different similarity scores (measure of nuclear translocation) in HC are shown adjacent to the violin plot. Cells were stained with the nuclear marker DAPI (blue), NFATc1 PE is displayed in magenta. (G) Quantification of

NFATc1 activation measure as absorbance at 450nm using an ELISA- based transcription factor activation assay on feeder expanded T-

lymphoblasts from patient or HC following stimulation with PMA/ionomycin. All experiments are representative of at least three independent experiments with similar findings, with the exception of unstimulated fraction of (G) where n=1. All data are mean \pm SEM and were analyzed by **two- way ANOVA with Bonferroni post hoc test (F)**, **one way ANOVA with Bonferroni post hoc test to correct for multiple comparison (G)**. WT, wild type. Scale bar= 5 μ m.

Figure 2. Dysfunctional NFATc1 impairs differentiation, effector function and survival of T cells. **(A)** Proportions of regulatory T helper (on the left) (Treg: CD3⁺CD4⁺CD25⁺FOXP3⁺) and T- follicular helper cells (on the right) (TFH: CD3⁺CD4⁺CD45RA⁻CXCR5⁺), in HCs (n=6) and patients (P1, P2) and **(B)** Proportions of naïve (CD45RA⁺CCR7⁺), T_{CM} (CD45RA⁻CCR7⁺), T_{EM} (CD45RA⁻CCR7⁻) or T_{EMRA} (CD45RA⁺CCR7⁻) subpopulations within CD4⁺ and CD8⁺ fractions. **(C)** Flow cytometry dot plots quantitating surface CD28 and CD57 expression on CD8⁺ T cells. **(D)** Summary bar graphs showing quantification of IL- 2 (Upper) or IFN- γ intracellular expression determined by flow cytometric analysis. (gMFI: geometric mean fluorescent intensity) T- lymphoblasts were analyzed for IL- 2 and IFN- γ production after 5 h of PMA/ionomycin stimulation and addition of Brefeldin A during the final 4 h. Surface staining was done with CD3, CD4 and CD8. **(E)** Flow cytometry plots showing the percentage of apoptotic cells in feeder expanded T- lymphoblasts, measured by Annexin- V and propidium iodide (PI) staining, after withdrawing IL- 2 from the growth media (upper plot) and following 24 hours treatment of IL- 2 (200IU/uL) (lower plot) **(F)** Summary bar graphs showing the percentage proliferation of the cells as measured by the dilution of the violet proliferation dye (VPD450) in CD4⁺ and CD8⁺ T cells from the patients and HCs after 3 days of stimulation with anti- CD3 soluble antibody, CD3/CD28 beads or phytohemagglutinin (PHA) **(G)** Summary bar graphs showing percentage of CD4⁺ and CD8⁺ T cells that have upregulated CD25 surface expression at day 3, corresponding to the proliferation experiments from (F) **(I)** Representative histogram showing CD25 expression normalized to mode of GFP+CD8⁺ T cells at day 3, corresponding to the experiments from (G) Summary plots of CD25 expression, following transfection of both patients' PBMCs are shown in the upper square within the graph. **(H)** Representative histogram showing the dilution of VPD450 in the GFP+ population of the patient CD8⁺ T cells transfected with either the GFP- NFATc1^{WT} (red) or GFP- empty

(blue) (EV:empty vector) plasmids at day 3, upon stimulation with CD3/CD28 beads.
Summary plots of the percentage

of proliferating cells, following transfection of both patients' PBMCs are shown in the upper square within the graph. **(J)** Flow cytometry histograms quantitating surface CD86 and CD25 expression on CD19 cells of the patients and HC following 48 hrs stimulation with CD40L and IL- 4 or CD40L and IL- 21. **(K)** Representative histogram showing the dilution of VPD450 in CD19 B- cells from the patients and HCs after 5 days of stimulation with CpG. **(L)** Representative flow cytometry plot showing Ca^{2+} influx in EBV transformed B lymphoblasts from P1, P2 and HC upon 100nM ionomycin treatment as measured by Ca^{2+} eFluor450 dye expression. All data are mean \pm SEM. **Statistical analysis for panels A, D, F and G was performed using a one- way ANOVA with Bonferroni post hoc test to correct for multiple comparison.**

Figure 3. Single- cell RNA sequencing reveals the altered transcriptomic profile of NFATc1- dysfunctional patients. Basal transcriptome and profiled the TCR repertoire of lymphocytes from P1 and P2 with that of controls utilizing single- cell RNA sequencing (5'- scRNAseq, 10x Genomics). **(A)** Analysis of T- cell receptor ab repertoire diversity with a tree- map representation for patients 1 and 2 and age- matched healthy controls. Each square represents a unique clone and its size reflects its productive frequency within the repertoire. **(B)** Uniform Manifold Approximation and Projection (UMAP) plot of the combined scRNA- seq dataset from the patients (P1- 2) and HCs. Left: Cells colored by cell type annotation after mapping to a reference data set of healthy PBMC⁶⁰ cell types with fewer than 20 cells omitted for clarity. Right: Cells colored by genotype; patients on top of HCs. **(C)** Bar graphs showing proportions of different cell populations within the lymphocytes. **(D)** Heatmap showing pseudobulk expression data for genes (shown as rows) that are differentially expressed between patients and controls within CD4⁺ and CD8⁺ T- cell populations (samples and cell types shown as columns). Genes shown are the top 20 up or down regulated in any of the two tests (tests performed with edgeR software with exact test and pseudobulk data, FDR < 0.05, ranked by p- value) Expression values shown are scaled log- counts per million cropped to the range - 2 to 2 **(E)** Heatmap showing single- cell expression data for genes differentially expressed between patients and controls within CD8⁺T- cell subpopulations (naïve, TCM and TEM). Genes shown are the top 30 up- or down- regulated in any of the three tests [tests performed as in panel

(D)]. **(F)** Heatmap showing single- cell pseudobulk

expression data for genes differentially expressed between patients and controls within CD19⁺ B- cells [tests performed as in panel (D)].

Figure 4. Altered epigenome landscape of patients' T- lymphoblasts. We performed an assay for transposase- accessible chromatin with high- throughput sequencing (ATAC- seq) on patient and HC T- lymphoblasts upon stimulation with PMA/ionomycin, to initiate downstream epigenetic and transcriptional changes **(A)** ATAC- seq chromatogram showing the accessibility of *IL2* gene locus in patients P1, P2 and HCs (n=2). Reads per genomic content (1x normalization, RPGC) normalized tracks. **(B)** Heatmap of differentially accessible regions at gene promoters (transcription start site +/- 1kb) between healthy control- derived (HC1, HC2) and patients- derived (P1, P2) expanded T cells (DESeq2; $\text{abs}(\log_2\text{FC}) > \log_2(1.3)$)⁶¹. Values are z- scores derived from 'regularized log' transformation (DESeq2 rlog function) of counts data. Positive values indicate that regions of the corresponding genes are more transcriptionally accessible, whereas negative values indicate that the regions are less accessible. **(C)** Heatmap of top 50 most significantly ($\text{padj} < 0.05$; a BH adjusted p- value for the variability being greater than the null hypothesis of 1) variable transcription factor motifs across samples of HC- derived (HC1, HC2) and patients- derived (P1, P2) expanded T cells. Values are z- scores for each bias corrected deviations. **(D)** Top 20 significantly ($\text{padj} < 0.05$; a BH adjusted corrected p- value ($p < 0.05$)) and HC- only enriched GOBP terms of genes associated with WT unique peaks.

Figure 5. Time course analysis of proliferation, activation and upregulation of checkpoint inhibitors of T cells in parallel to RNA sequencing reveals their delayed responses associated with perturbed metabolism. **(A)** Representative histograms showing the percentage of CD4⁺ or CD8⁺ T cells with upregulated CD25 surface expression after stimulation with CD3/CD28 beads and percentage of proliferation by measuring dilution of the VPD450 in CD4⁺ and CD8⁺ T cells from patients and 3 HCs at basal state (unstimulated), day 1, day 2, day 3, day 4, day 7 and day 10 after stimulation. Marker up/downregulation was measured by flow cytometry at basal state (before stimulation), day 1, day 2, day 3, day 4, day 7 and day 10 after stimulation. **(B)** Summary graphs showing the percentage of CD8⁺ T cells that have upregulated PD1, LAG3, AITR/GITR surface expression after stimulation with

CD3/CD28 beads measured by flow cytometry at basal state (unstimulated), day 1, day 2,

day 3, day 4, day 7 and day 10 after stimulation. **(C)** PBMCs from patients and 4 HCs were stimulated with CD3/CD28 beads and on the 3rd day after stimulation CD8⁺ T cells were sorted by flow cytometry. Bulk RNA sequencing was performed on sorted CD8⁺ T cells. Plots show the gene set enrichment analysis (GSEA) of 50 “hallmark” functions based on calculated normalized enrichment score. Pathways are stratified for the top 10 most significantly upregulated pathways upon stimulation comparing the patients and the HCs **(D)** Plots showing the calculation of ranking of normalized enrichment score (NES) within geneset enrichment analysis (GSEA) from Hallmark database representing the stimulation induced changes in expression of CD8 T cells in the patients and healthy controls with regards to oxidative phosphorylation (right) and glycolysis genesets (left). **(E)** Heatmap showing the expression of genes involved in glucose metabolism extracted from bulk RNA- sequencing analysis. Significance for gene expressions are indicated in the figure legend.

Figure 6. Metabolic profiling of NFATc1- dysfunctional T cells shows the impaired glycolysis upon stimulation. (A) Summary dot plots showing the ratio of change of expression level of Glucose transporter 1 (GLUT1) and glucose uptake using fluorescent glucose analog 2- [N- (7- nitrobenz- 2- oxa- 1,3- diazol- 4- yl) amino]- 2- deoxy- D- glucose (2- NBDG) following 24- hour stimulation of feeder expanded T cells with soluble CD3/CD28 antibodies measured by gMFI **(B)** Extracellular flux analysis. Above: Graph showing oxidative consumption rate (OCR) of HC (n=3) and patients' CD8⁺ T- lymphoblasts following 30 min stimulation with CD3/CD28 beads and subjected to mitochondrial stress test. Below: Graph showing extracellular acidification rate (ECAR) of HC (n=3) and patients' CD8⁺ T- lymphoblasts which were stimulated for 30 min with CD3/CD28 beads and subjected to glycolytic stress test. Experimental data were normalized to flow cytometric cell counts. FCCP: Carbonyl cyanide- p- trifluoromethoxyphenylhydrazone, Oligo: Oligomycin, Rot: Rotenone, AA: Antimycin A. **(C)** Upper panel: Immunoblot showing the protein expression levels of Hexokinase- 2 (HK2), glucose transporter- 3 (GLUT3), Carnitine palmitoyl transferase 1a (CPT1a), Glyceraldehyde 3- phosphate dehydrogenase (GAPDH), lactate dehydrogenase (LDH) on patient and HC T- lymphoblasts following 24 hour stimulation with soluble anti- CD3/CD28 antibodies. Lower panel: Graphs showing the quantification of the

Western blots averaged from 3 independent experiments displaying the expressions of HK2 and CPT1a. **(D)** Scheme summarizing the metabolic alteration observed in patient T- lymphoblasts following stimulation. **(E)** Heatmap

showing fold changes of metabolite concentrations (stimulated/unstimulated) in T-lymphoblasts in patients and HCs measured by metabolomics following 24 hours of stimulation with soluble anti CD3/CD28 antibodies. All data are mean \pm SEM. **Statistical analysis was performed using one- way ANOVA with Bonferroni post hoc test (A and B) or two- way ANOVA with Bonferroni post hoc test (C) to correct for multiple comparison.**

Figure 7. Shifted substrate preference towards fatty acid oxidation in NFATc1-dysfunctional T cells. **(A)** Summary dot plot showing the lipid uptake of patient and HC T- lymphoblasts following 24 hours stimulation with soluble anti- CD3/CD28 antibodies using Bodipy FL C16 staining. **(B)** Bar graph showing the measured levels of total lipid species in healthy controls and patients with and without stimulation **(C)** Volcano plot showing the log₂ fold changes (x- axis) in lipid species upon stimulation in healthy controls versus patients. y- axis represents the p values for negative log₁₀ of the measurements. Red full circles represent the TAG species, each significantly changed TAG species is indicated (Statistics performed using Student's t tests) **(D)** Heatmap showing fold changes in concentrations of different lipid species in patient and HC T- lymphoblasts measured by mass spectrometry based lipidomics following 24 hours of stimulation with soluble anti- CD3/CD28 antibodies. **(E)** Scheme depicting the TCA cycle and the TCA cycle intermediates that are detected in the current analysis. Summary graphs show the relative ¹³C enrichment of TCA cycle intermediates in patient T lymphoblasts incubated in [U- ¹³C₁₆] palmitate normalized to the HCs. **(F)** SCENITH analysis showing the metabolic alterations of patients (P1- P2) and HC (experiment 1:n=4; experiment 2:n=3) CD8⁺- TEM population following CD3/CD28 beads stimulation. The experiment is performed twice and the plot shows the averaged results from each experimental replicate. The negative percentage values shown in the graph inherent to the analysis of the assay. The calculations formulas are indicated in the methods section. **Statistical analysis was performed using two- way ANOVA with Bonferroni post hoc test to correct for multiple comparison.**

We treated the sorted naïve T cells from HCs (n=4) and treated them with vehicle, cyclosporin A (300 nM) or 2- deoxyglucose (1 μ M) and stimulated them with DynaBeads coated with CD3 and CD28 antibodies: **(G)** Summary graphs showing the percentage of CD8⁺ T cells with upregulated CD25 surface expression after stimulation with CD3/CD28

DynaBeads and percentage of proliferation by measuring dilution of the VPD450 in CD8⁺ T

cells from at basal state (unstimulated), day 2, day 3, day 4, and day 8 after stimulation in vehicle or CsA or 2DG treated . Summary graphs showing the geometric mean fluorescent intensity (gMFI) of 2NBDG and Bodipy FL16 in CD8⁺ T cells after stimulation with CD3/CD28 beads measured by flow cytometry at basal state (unstimulated), day 2, day 3, day 4, and day 8 after stimulation. **(H)** Left panel: Immunoblot showing the protein expression levels of Hexokinase- 2 (HK2), Carnitine palmitoyl transferase 1a (CPT1a), Glyceraldehyde 3- phosphate dehydrogenase (GAPDH), Right panel: Graphs showing the quantification of the Western blots averaged from 3 independent experiments displaying the expressions of HK2 and CPT1a on HC naïve T cells harvested on day 4 following stimulation with DynaBeads. **(I)** Summary graphs show the relative ¹³C enrichment of TCA cycle intermediates (citrate, malate, aspartate) in HC T cells stimulated with DynaBeads (for 4 days) and treated with CsA or 2DG or vehicle, incubated in [U- ¹³C₁₆] palmitate normalized to the vehicle treatment. (All data are mean ± SEM. Statistics performed using with one way ANOVA with post hoc Bonferroni correction if not stated otherwise.)

Figure 1

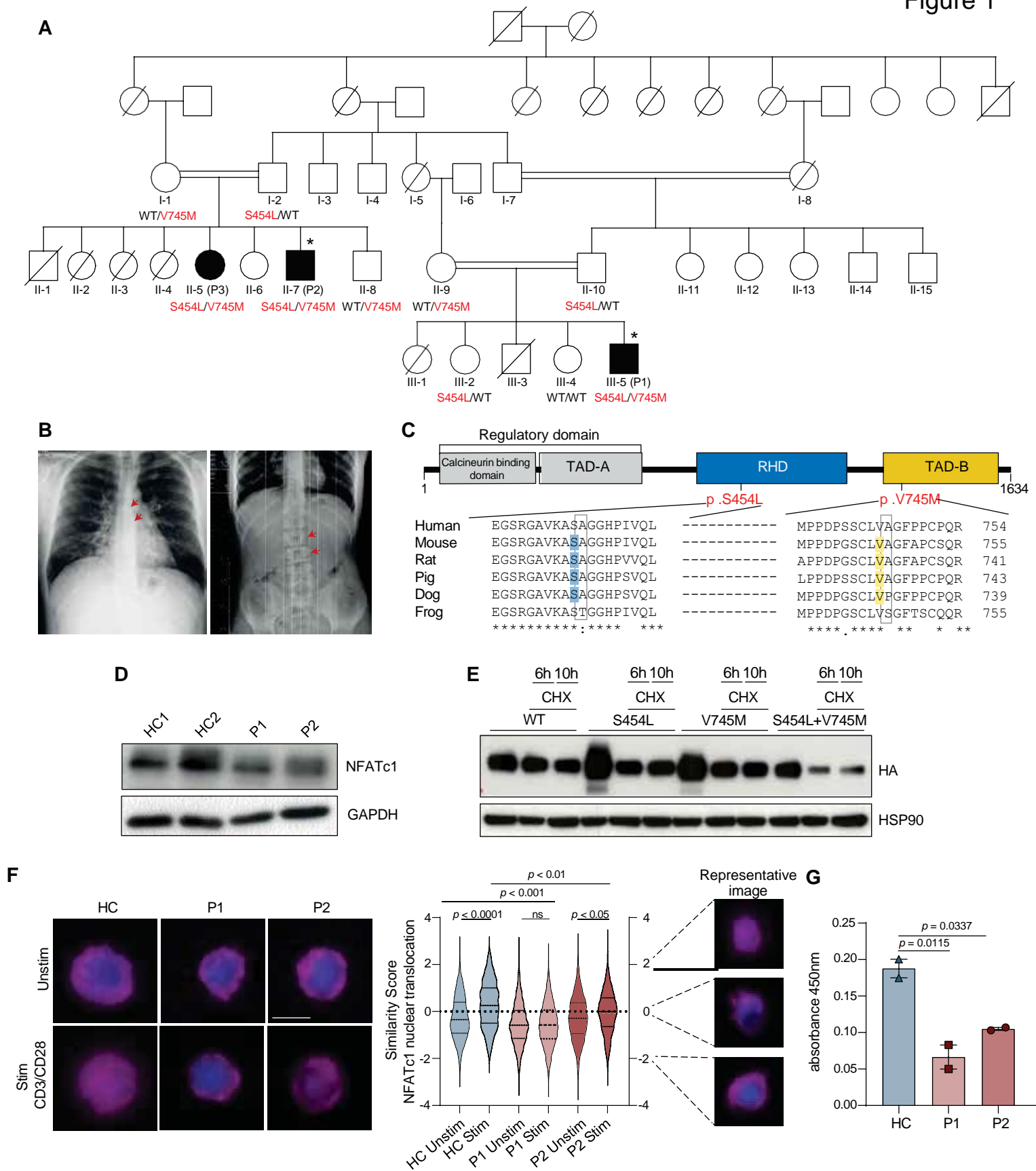


Figure 2

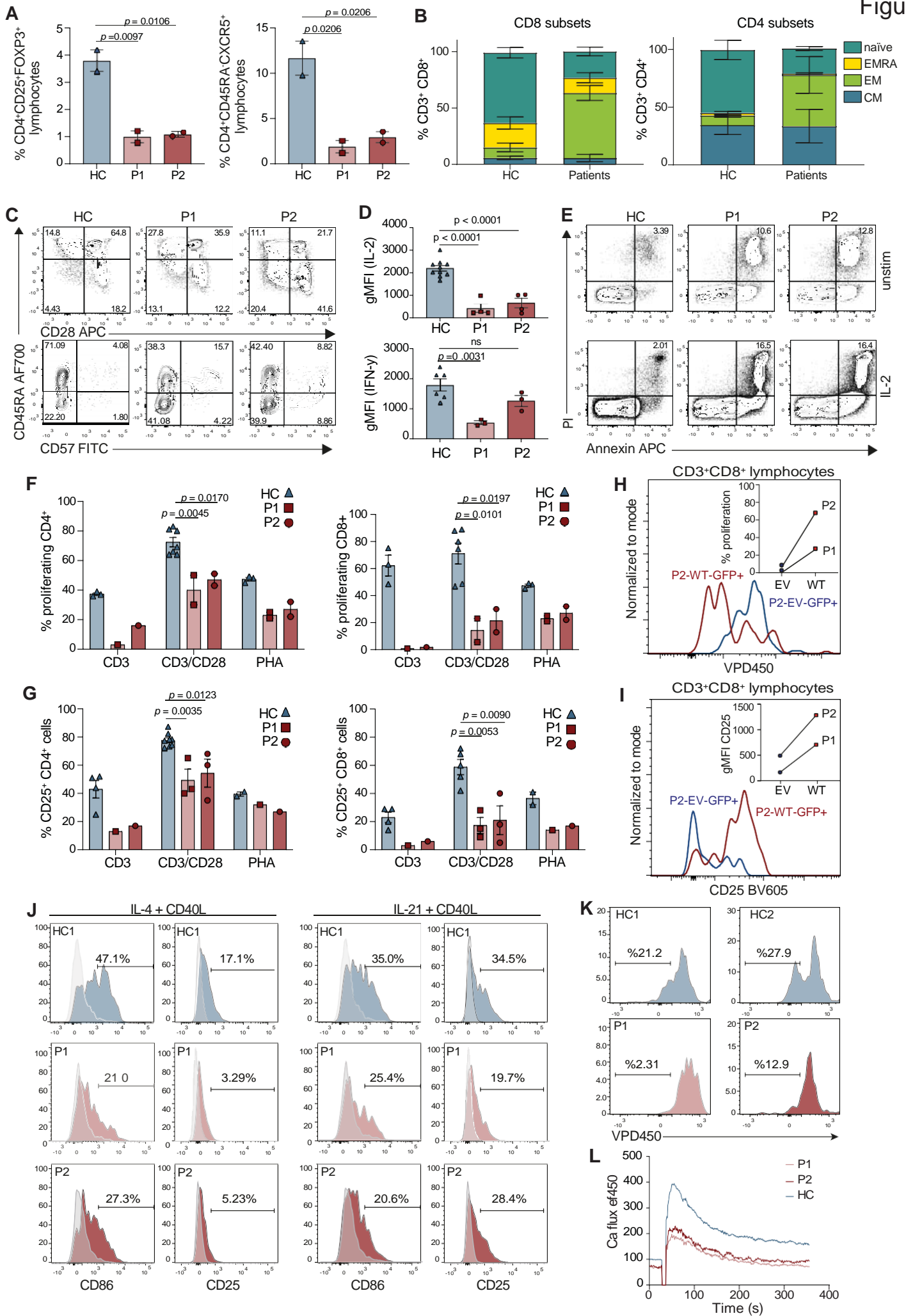


Figure 3

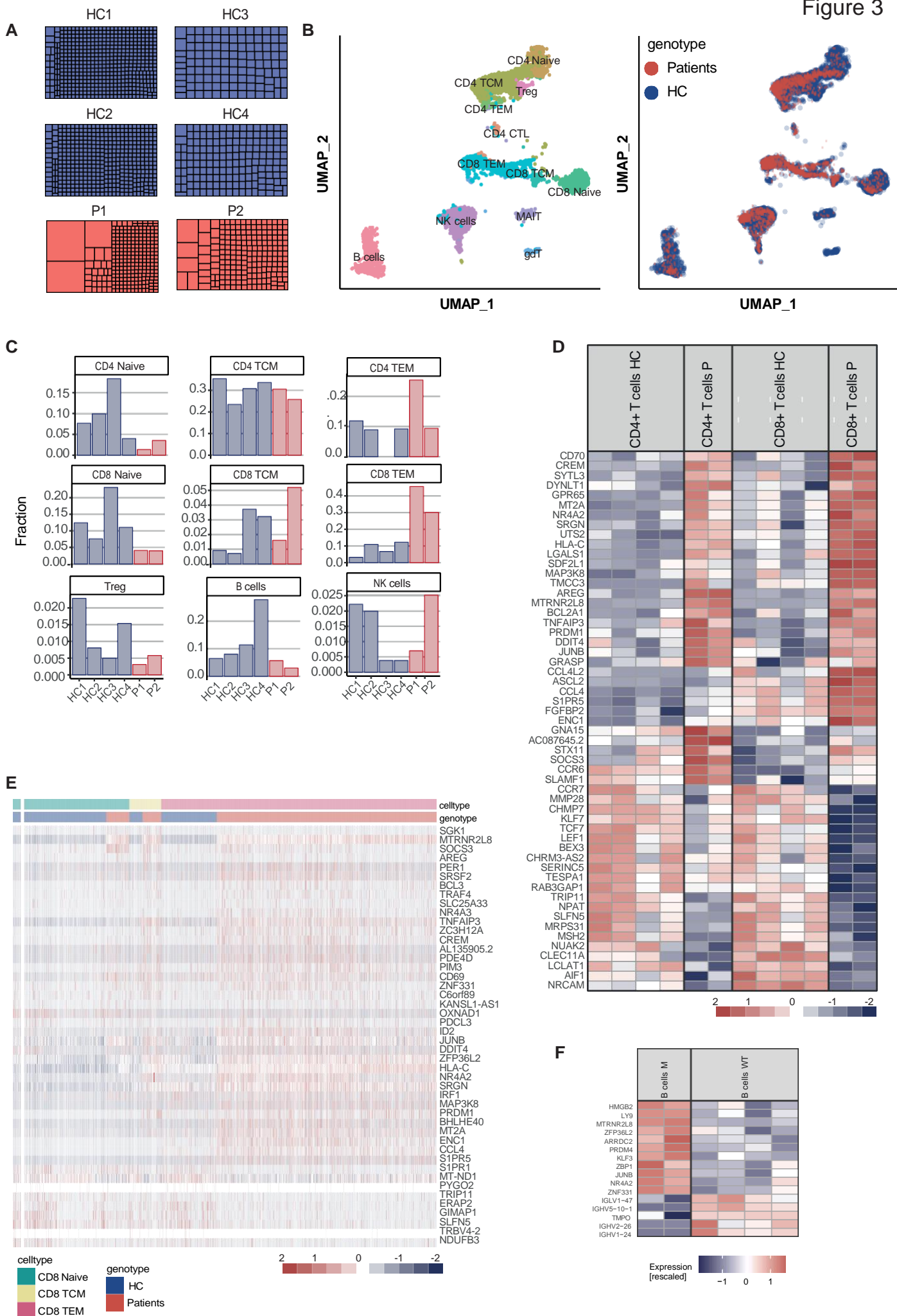


Figure 5

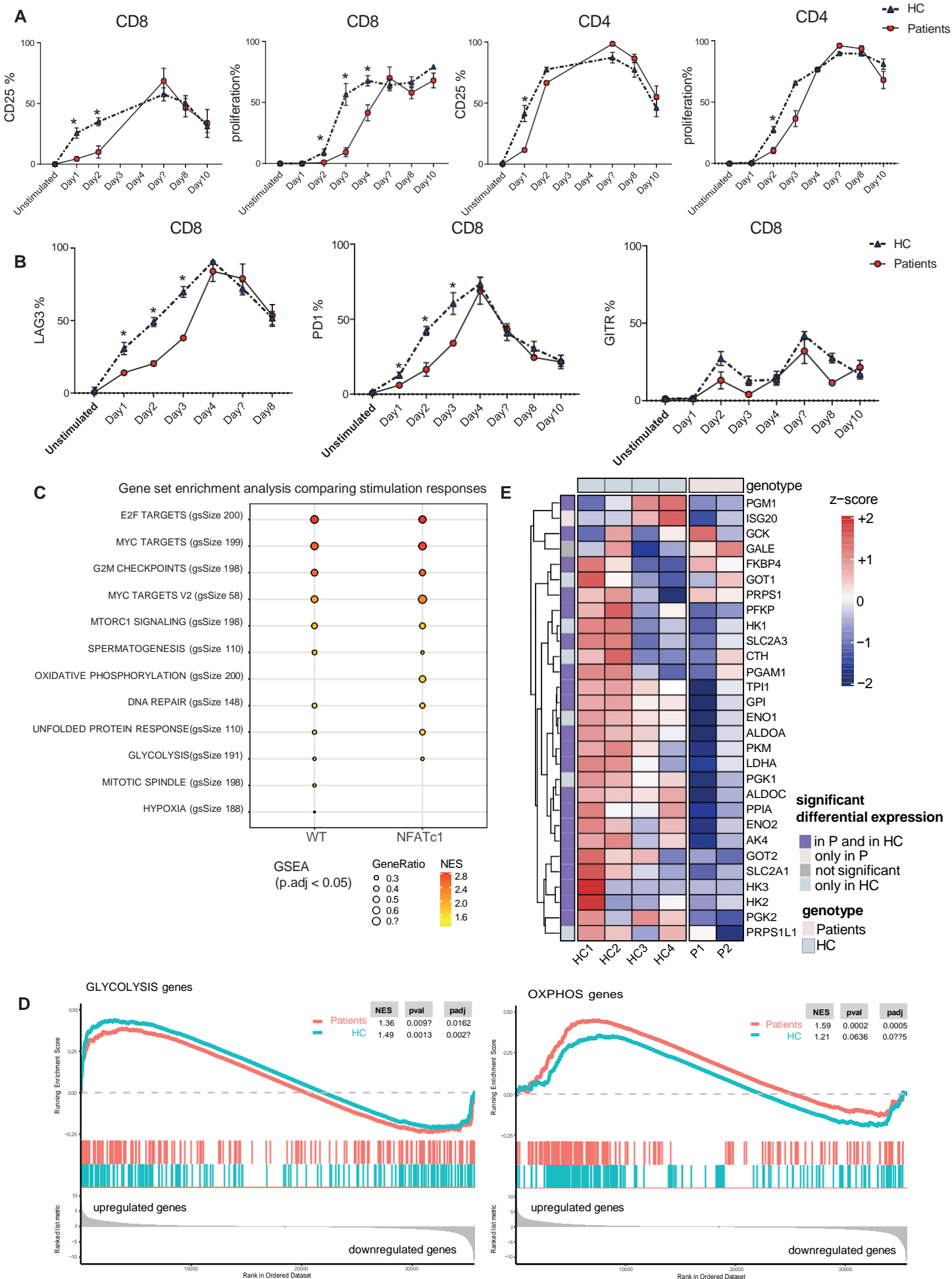


Figure 6

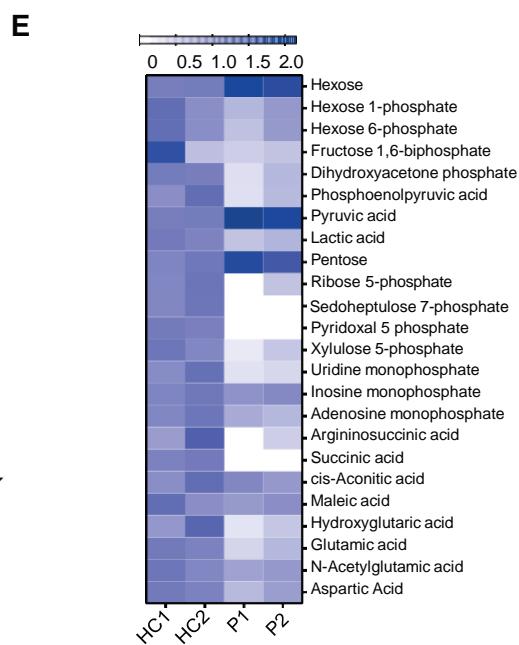
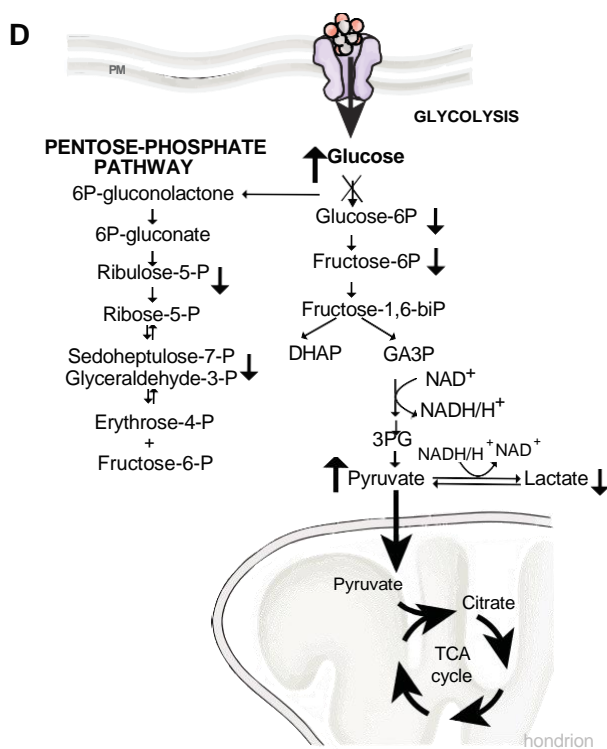
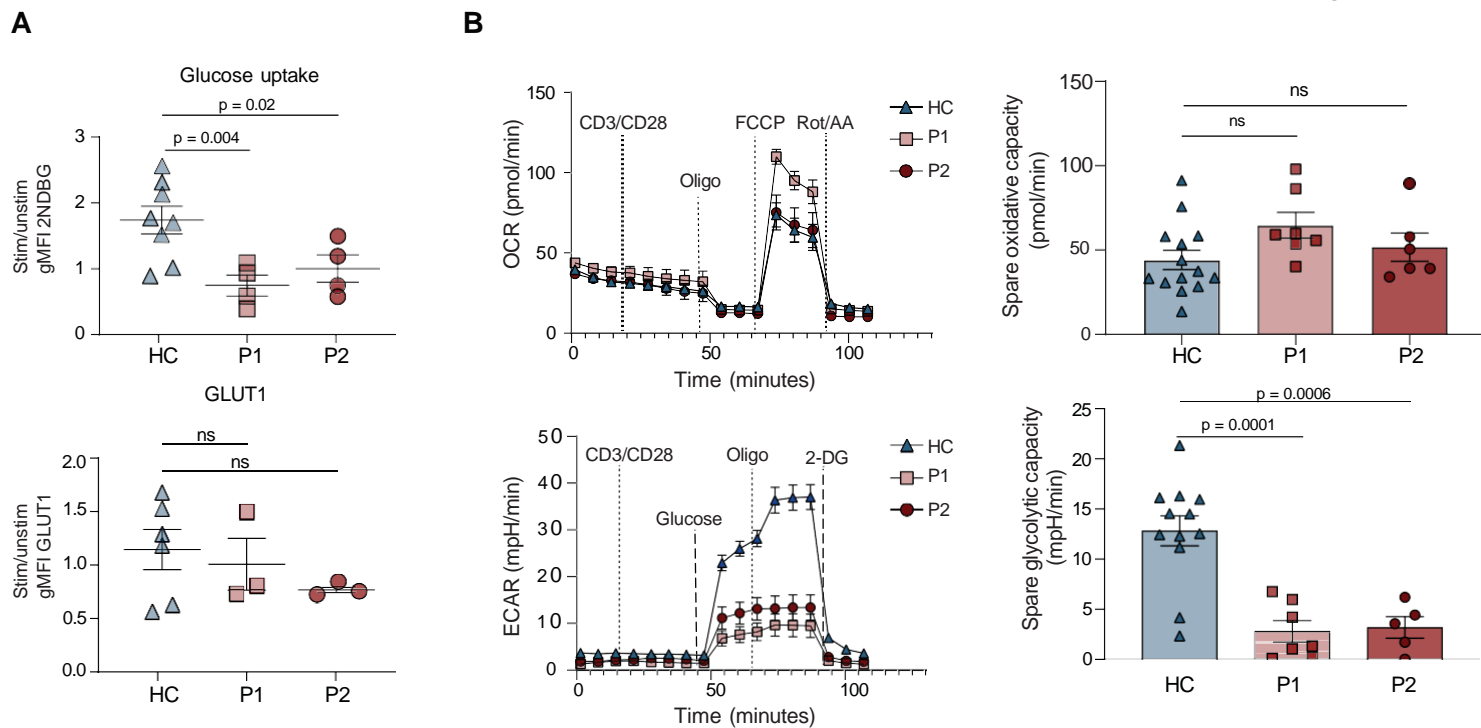


Figure 7

